AFRL-VS-TR-2003-1559

TWO MODELS FOR PREDICTING THE PROBABILITY OF A CLOUD-FREE LINE-OF-SIGHT

Susan A. Triantafillou
Guy P. Seeley

Radex, Inc.
Three Preston Court
Bedford, MA 01730

8 November 2002

Scientific Report No. 6

APPROVED FOR PUBLIC RELEASE; DISTRIBUTION UNLIMITED

AIR FORCE RESEARCH LABORATORY
Space Vehicles Directorate
29 Randolph Road
AIR FORCE MATERIEL COMMAND
Hanscom AFB, MA 01731-3010

"This technical report has been reviewed and is approved for publication"

/signed/

FRANK GIBSON
Contract Manager

/signed/

ROBERT BELAND
Branch Chief

This report has been reviewed by the ESC Public Affairs Office (PA) and is releasable to the National Technical Information Service (NTIS).

Qualified requestors may obtain additional copies from the Defense Technical Information Center (DTIC). All others should apply to the National Technical Information Service (NTIS).

If your address has changed, if you wish to be removed from the mailing list, or if the addressee is no longer employed by your organization, please notify AFRL/VSIM, 29 Randolph Road, Hanscom AFB MA 01731-3010. This will assist us in maintaining a current mailing list.

Do not return copies of this report unless contractual obligations or notices on a specific document require that it be returned.

REPORT DOCUMENTATION PAGE

Form Approved
OMB No. 0704-0188

1. AGENCY USE ONLY (*Leave Blank*)	2. REPORT DATE	3. REPORT TYPE AND DATES COVERED
	8 November 2002	Scientific Report No. 6

4. TITLE AND SUBTITLE

Two Models for Predicting the Probability Of a Cloud-free Line-of-sight

5. FUNDING NUMBERS

PE 61102 F
PR S321 TA GY WU AG

Contract F19628-98-C-0010

6. AUTHORS
Susan A. Triantafillou
Guy P. Seeley

7. PERFORMING ORGANIZATION NAME(S) AND ADDRESS(ES)
Radex, Inc.
Three Preston Court
Bedford, MA 01730

8. PERFORMING ORGANIZATION REPORT NUMBER

RXR-02-1001

9. SPONSORING / MONITORING AGENCY NAME(S) AND ADDRESS(ES)
Air Force Research Laboratory
29 Randolph Road
Hanscom AFB, MA 01731-3010
Contract Manager: F. Gibson/VSBL

10. SPONSORING / MONITORING AGENCY REPORT NUMBER

AFRL-VS-TR-2003-1559

11. SUPPLEMENTARY NOTES

12a. DISTRIBUTION / AVAILABILITY STATEMENT

Approved for Public Release; Distribution unlimited

12b. DISTRIBUTION CODE

13. ABSTRACT *(Maximum 200 words)*

Two modeling approaches are proposed to predict the probability of a cloud-free line-of-sight (PCFLOS) from space-borne sensor to a missile or other object. The models, which account for various cloud conditions and zenith angles, are suitable for military training and simulation purposes. One approach uses a set of detailed models to generate a cloud scene and randomly place missiles within it. A simulated sensor then detects the missiles to which it has a CFLOS and the fraction detected is interpreted as the PCFLOS. The second approach is a simplified model that constructs two-dimensional scenes containing rectangular clouds. The fraction of area that remains visible between clouds from a collection of scenes is the PCFLOS. This calculation relies on cloud metrics that are evaluated in consideration of meteorological observations and then tuned to improve agreement with the detailed model. The detailed model approach is computationally expensive, but can be used to precompute a range of values, from which a required PCFLOS can be interpolated. The simplified model is computationally inexpensive and easy to implement, however it requires a set of detailed model results for tuning purposes.

14. SUBJECT TERMS
Line-of-sight, Cloud-free line-of-sight, Missile detection, Obscuration by clouds, Cloud model

15. NUMBER OF PAGES

16. PRICE CODE

17. SECURITY CLASSIFICATION OF REPORT	18. SECURITY CLASSIFICATION OF THIS PAGE	19. SECURITY CLASSIFICATION OF ABSTRACT	20. LIMITATION OF ABSTRACT
Unclassified	Unclassified	Unclassified	Unlimited

CONTENTS

LIST OF FIGURES

ACKNOWLEDGMENTS

The authors would like to thank Dr. Joel B. Mozer of the Air Force Research Laboratory for supporting this project. Gratitude is given to Capt. A. Eckel and Capt. J. Crane of Schriever AFB, CO for their input and their numerical experiments with the detailed model. We would also like to thank David J. Smalley of Sencom for helping to characterize cloud dimensions for the visible area model and for his assistance with detailed model calculations. And finally we thank Sara C. Gordon of Radex, Inc. for applying the hypercube program to this study.

1. INTRODUCTION

Space-based missile detection systems must contend with the presence of atmospheric clouds in the troposphere. For a surveillance system designed to detect airborne missiles, particularly those in boost phase, clouds in the line-of-site may obscure, or completely mask the target when viewed from above. The nature of atmospheric clouds is a significant variable in such a mission. Clouds can occur at altitudes from the ground to more than 15 km and range from transparently thin to many kilometers thick. Perhaps most variable is the spatial distribution of clouds, often characterized as the fraction of the sky that the clouds occupy, when viewed from the ground, and their taxonomy (i.e. cirriform, cumuloform, and stratiform) which generally describes their shape and texture.

All of these cloud characteristics must be considered in order to quantify the effect of clouds on space-based surveillance missions. For training, or other modeling purposes, it is desirable to construct realistic synthetic simulations of the environment in which a missile detection system must operate. Due to the highly complex physical nature of clouds and their relationship to weather conditions and local climatology, it is generally not practical to model detailed cloud fields directly in such simulations. Rather, it is often required that the effects of clouds on the surveillance system be modeled as a function of simple, descriptive inputs such as cloud-base altitude, top altitude, type, and coverage. A convenient output of such a model is the probability of the existence of a cloud-free line-of-sight (PCFLOS) between the target and the surveillance sensor based on these cloud parameters and the three-dimensional locations of the target and sensor.

A model proposed by *Eckel* [1999] uses a simple calculation to predict PCFLOS based on supposition. The model reflects the assumptions that PCFLOS decreases with look angle and cloud thickness. The model produces sensible results that are useful for training, but lacks a physical basis and has not been compared to actual PCFLOS measurements or the results of a physically based model. A goal of the present work is to use a detailed model to generate PCFLOS values for comparison with Eckel's results. In addition, a simple, physically based model to predict PCFLOS is desired. This would serve as a fast means of estimating PCFLOS and a tool for understanding the impact of cloud thickness and cloud coverage on PCFLOS. Ideally, all of the models could be judged against actual PCFLOS measurements.

The detailed model is comprised of three components used in sequence. First, a cloud scene is generated by the Cloud Scene Simulation Model (CSSM) described in [*Cianciolo*, 1992; 1996] and [*Turkington*, 1998]. Next, the radiative properties of the cloud elements in the scene are evaluated by a tool called Fastmap [*Cianciolo*, 1996]. Finally, a model called tmodel examines lines-of-sight to a large number of randomly placed missiles to determine PCFLOS for the scene. The PCFLOS values determined by this detailed approach are generally lower than those of the Eckel model for moderately thick clouds.

The fast, simple model proposed here generates fictitious cloud scenes and then calculates the average visible area for a specified zenith angle. To keep the model simple, it is necessary to make many assumptions about the clouds, particularly the shapes and characteristic aspect ratios of

clouds. It is shown that these assumptions can be made in accordance with meteorological observations so that the simplified model results agree with detailed model results.

This report is organized as follows: The detailed approach, along with the associated results, are given in the next section. This is followed by a section describing the simplified model and its results. The section contains a discussion of the geometry of the PCFLOS problem, which is the basis of the simplified model. This discussion is instructive in understanding the results of both the detailed and simplified models. For convenience of computation, the simplified model is summarized in the Appendix. Actual PCFLOS measurements are discussed in Section 4. Section 5 contains concluding remarks.

2. DETAILED MODEL

2.1 Model Description

A series of detailed models is used to predict PCFLOS based on physical and empirical arguments. These models generate a cloud scene, evaluate its radiative properties, and determine the probability of detecting missiles below the cloud deck from different zenith angles above the cloud deck. Results of several different cloud scenes are combined to produce the PCFLOS for a fixed cloud coverage and cloud thickness. This simulation tool is made up of the three models described below.

Synthetic clouds are rendered using the Cloud Scene Simulation Model (CSSM), described in [*Cianciolo*, 1992; 1996] and [*Turkington*, 1998]. The CSSM populates a volume with clouds according to user specified input, including cloud coverage, base, and top. An outcome of the CSSM is the cloud liquid water content (CLWC) throughout the volume. The model was designed to produce CLWC that is statistically similar to that measured in real clouds along flight paths. The CSSM is based on a fractal algorithm which meets this CLWC requirement while generating realistic-looking clouds. An input to the algorithm is a five-digit random number seed which allows the CSSM to produce a large number (100,000) of different cloud scenes for a single set of meteorological input data. The meteorological data includes a sounding, as well as cloud coverage, base, thickness, and type.

From the CLWC information produced by CSSM, relevant radiative properties of the volume are computed using a model called Fastmap, which is described in detail in [*Cianciolo*, 1996]. Fastmap uses precomputed lookup tables to convert CLWC fields into optical properties based on assumptions of drop size distribution. Fastmap is applied here to obtain extinction coefficients throughout the volume.

The extinction coefficients are used by an imaging tool called tmodel. Tmodel loads a three-dimensional field into an OpenGL texture map for rendering on an SGI workstation that is equipped with texture-mapping hardware. The grid cells in the field that are clouded are those that have extinction coefficients above a selected threshold, which effectively renders clouds as opaque.

Tmodel introduces missiles, one at a time, into the image and determines which missiles are detectable to a sensor above the cloud deck.

For a zenith angle of 0° the clouds, the missiles, and the sensor are positioned relative to an origin, as shown in Figure 1. The sensor altitude can be several orders of magnitude greater than the missile and cloud altitudes. For this reason, Figure 1 shows the area around the sensor and the area around the clouds while omitting the area in between. The cloud volume is centered over the origin. Tmodel randomly distributes missiles, rendered as spheres, at a user-specified altitude and within a horizontal rectangle aligned with the cloud volume. The sensor views the region at a fixed distance from the origin and through an opening angle chosen to capture the entire cloud base when the sensor is directly above the clouds. If the line-of-sight to a missile is not obscured by cloud elements then the missile is detected. Each missile is removed before another is introduced.

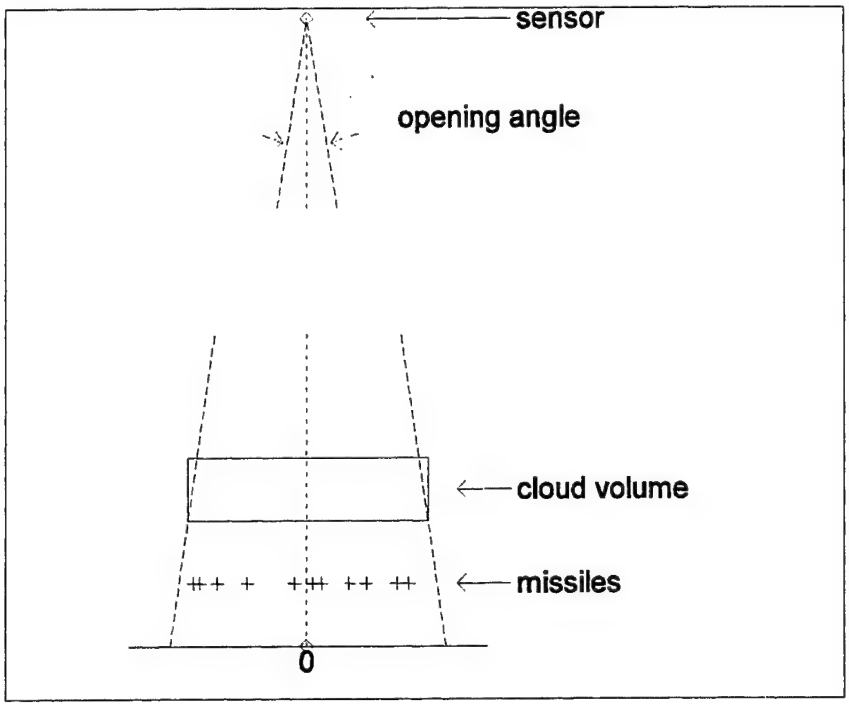

Figure 1. Tmodel Geometry for 0° Zenith Angle.

For zenith angles greater than 0°, the sensor position maintains the same opening angle and distance from the origin that are used for viewing at a 0° zenith angle. The sensor's view encompasses an area larger than the cloud volume centered over the origin, as in the example shown in Figure 2. To assure that lines-of-sight go through the cloud deck, several copies of the cloud volume are tiled in a row. For example, in the case of Figure 2, two tiles are required to assure that all possible lines-of-sight between the sensor and the missiles go through the full thickness of the cloud deck. The number of tiles required is dependent on distance to the sensor, tile width, cloud base, cloud thickness, and maximum zenith.

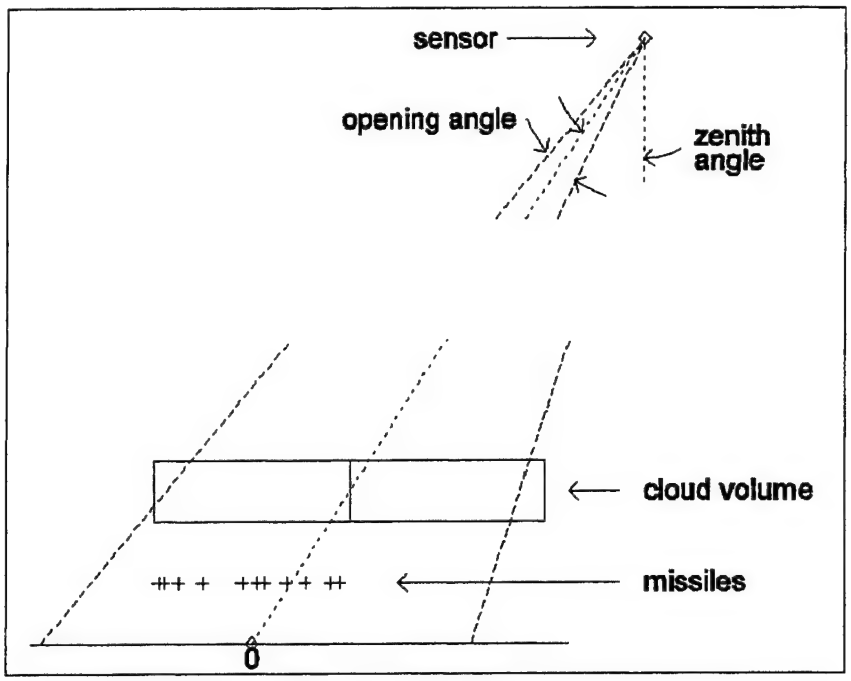

Figure 2. Tmodel Geometry for Nonzero Zenith Angle.

Once tmodel has processed all of the missiles for a particular zenith angle, it produces the fraction of missiles that have been detected. This is interpreted as PCFLOS for a given cloud scene. Results for several scenes are averaged together to represent variations in PCFLOS that occur with different cloud arrangements.

Computing average PCFLOS for a single cloud coverage, cloud thickness, and zenith angle is a time-consuming process, requiring several minutes of computation. Most of this time is due to the tmodel portion of the calculation. In order to obtain faster results based on this detailed approach, PCFLOS results for selected input values are precomputed and stored in a ``hypercube." A hypercube is a multi-dimensional array of data from which values can be linearly interpolated. It can return thousands of results per second. The hypercube is used here for a three-dimensional array of PCFLOS values. The dimensions are spanned by cloud coverage, cloud thickness, and zenith angle.

2.2 Model Results

The detailed model and the hypercube are implemented for a limited set of input values. This section specifies the cases used and shows the resulting PCFLOS values. Use of the hypercube for cases that are not specifically computed by the detailed model is demonstrated.

The CSSM and Fastmap are applied to a rectangular volume that is 4.0 km on each horizontal side and 6.0 km high and is positioned 0.1 km above the ground. For all cloud scenarios, stratocumulus clouds with bases at 0.5 km and thicknesses of 0.5, 1.5, 2.5, 3.5, 4.5, and 5.5 km are used. Other

meteorological data is due to a sounding from 12 May 1997 at Hanscom Air Force Base, MA. The clouds are represented on a grid with 64 x 64 x 64 grid cells. The cloud coverages considered are 20, 40, 60, and 80 percent. The range of cloud coverage is extended by assigning a PCFLOS of 1.0 for cases with 0 percent coverage and 0.0 for 100 percent coverage. These input values are expected to be at suitable intervals for use of the hypercube.

Tmodel simulates a sensor positioned 1000 km from the origin with a 0.23° opening angle. Three thousand missiles, represented by 0.02 km diameter (less than 3 pixels) spheres are placed at an altitude of 0.2 km. Calculations are done for thirty different zenith angles: 0.5°, 2.5°, ..., 58.5°. For a zenith angle of 0° the PCFLOS is assumed to be one minus the coverage. Four cloud tiles are used, since four are required for the higher zenith angles.

The results of four different cloud scenes are averaged to represent each set of cloud coverage and cloud-base values. This number is selected based on numerical experimentation showing no significant change in average PCFLOS results when the number of cloud scenes is increased from three to four. The fact that the average value stabilizes suggests that four scenes provides sufficient representation.

Figure 3 shows PCFLOS results for four individual scenes for the case of 20 percent coverage and 0.5 km thickness. This example shows substantial variations in PCFLOS for the different scenes. Variation even occurs for a 0° zenith angle, where the PCFLOS is expected to be one minus the coverage, or 0.80. This result is typical and even greater variations occur at 0° zenith for some cases, suggesting that CSSM fails to produce the coverage as specified.

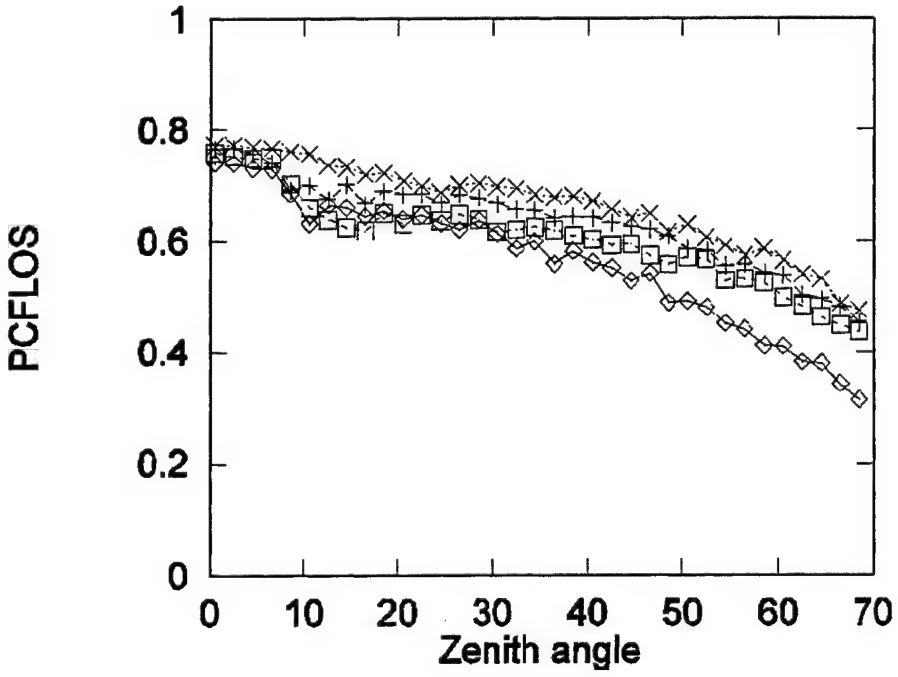

Figure 3. Tmodel Results for Four Cloud Scenes Representing 20 Percent Coverage, 0.5 km Thickness.

Another feature of Figure 3 is the increase in PCFLOS with zenith angle that occurs for some of the scenes when the zenith angle is about 15°. This indicates that the cloud configurations are favorable to viewing at that zenith angle. This will be discussed further in Section 3.1. It is unusual to see several cloud scenes exhibiting this feature for the same zenith angle.

Figure 4 shows the average values for the scenes represented in Figure 3. Averaging four results reduces the impact of atypical features, such as an increase in PCFLOS at a particular zenith angle. It also helps reduce errors, such as incorrect cloud coverage, that occur in some individual scenes.

Average PCFLOS values for many cases are shown in Figures 4 through 11. These figures also show standard deviations due to the different scenes and PCFLOS results of the Eckel model. In many low-coverage cases the standard deviations are large and are associated with PCFLOS differences of up to 0.4 between different cloud scenes representing the same input values. While it is reasonable for two cloud scenes to differ greatly, it suggests a need to incorporate more than four cloud scenes into the calculation.

A significant difference between the results of the detailed and Eckel models is the detailed model's faster drop-off in PCFLOS with increasing zenith angle that occurs for thicker cloud cases. Note that the Eckel model was designed to capture such a drop-off but only for much thicker clouds.

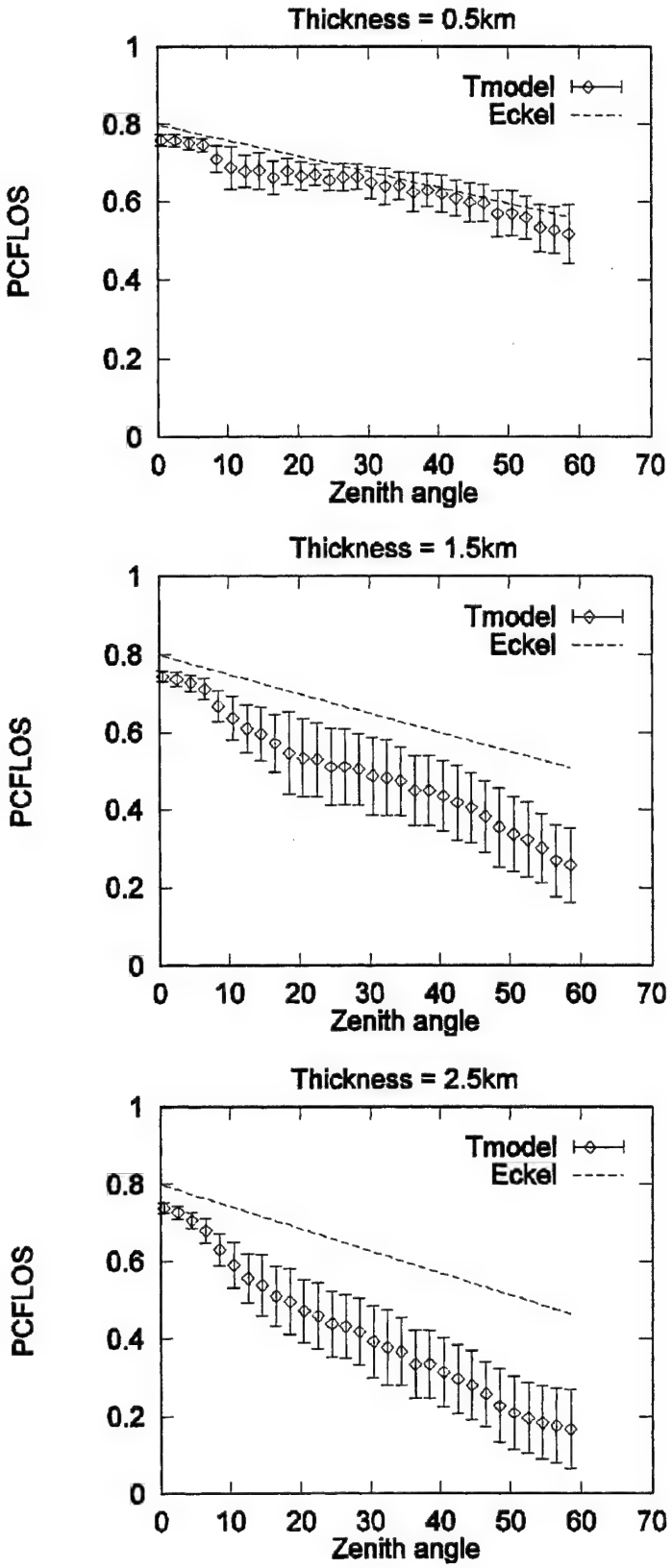

Figure 4. Tmodel Results for 20 Percent Coverage of Thin Clouds.

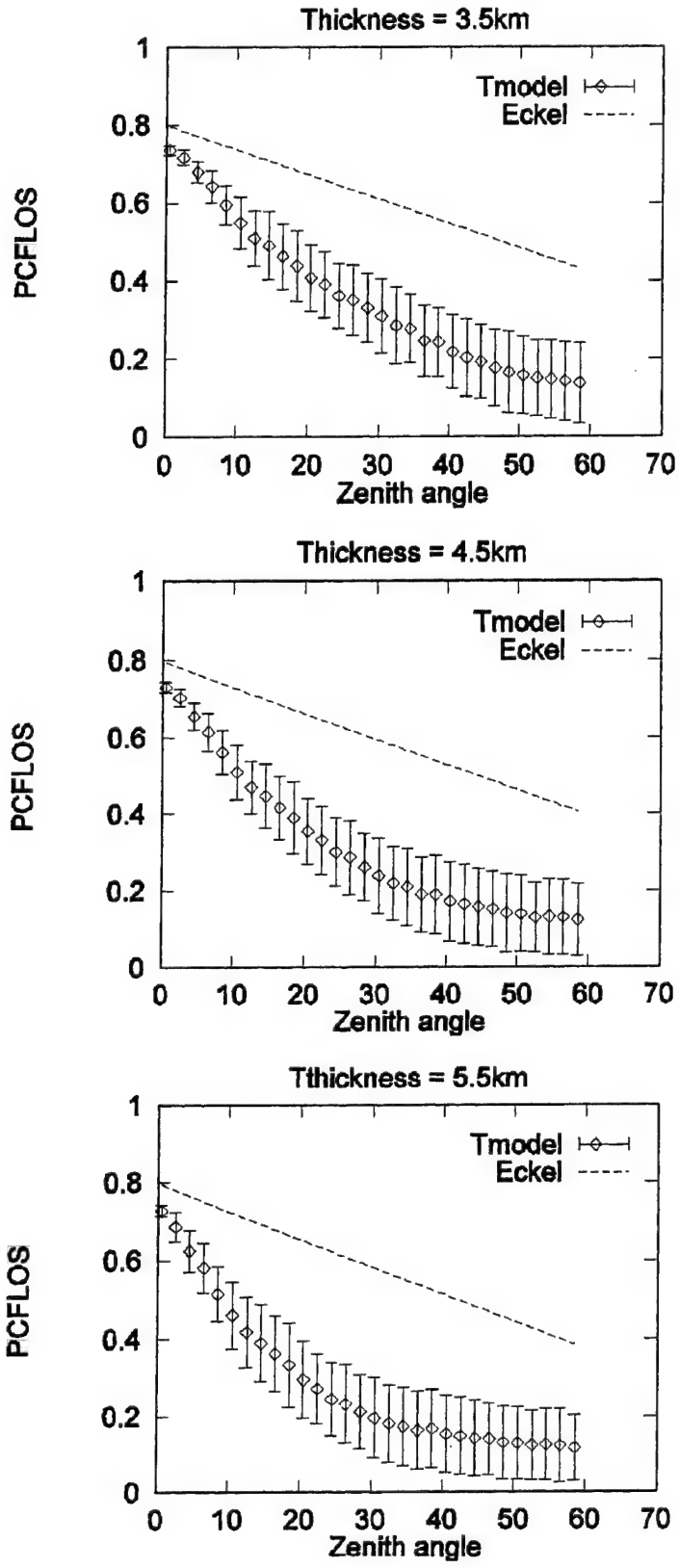

Figure 5. Tmodel Results for 20 Percent Coverage of Moderately Thick Clouds.

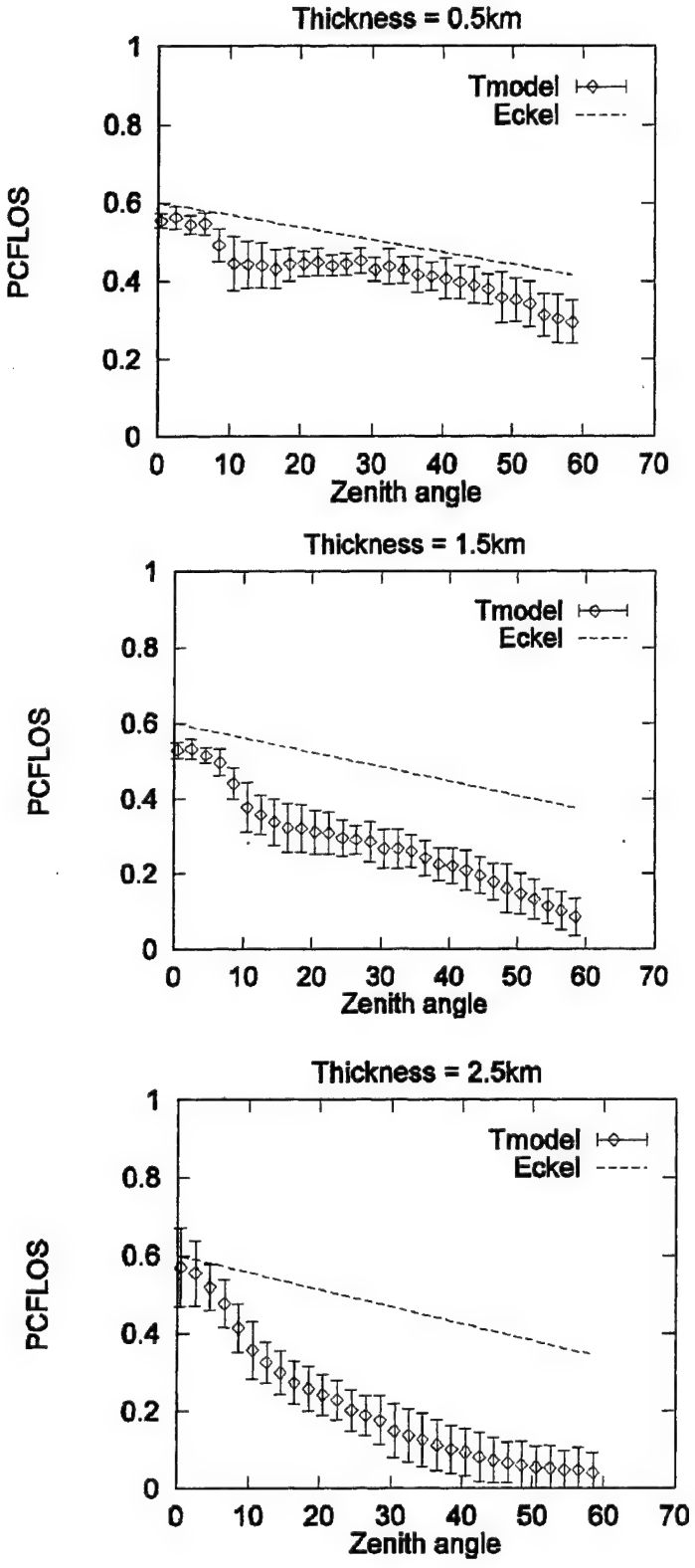

Figure 6. Tmodel Results for 40 Percent Coverage of Thin Clouds.

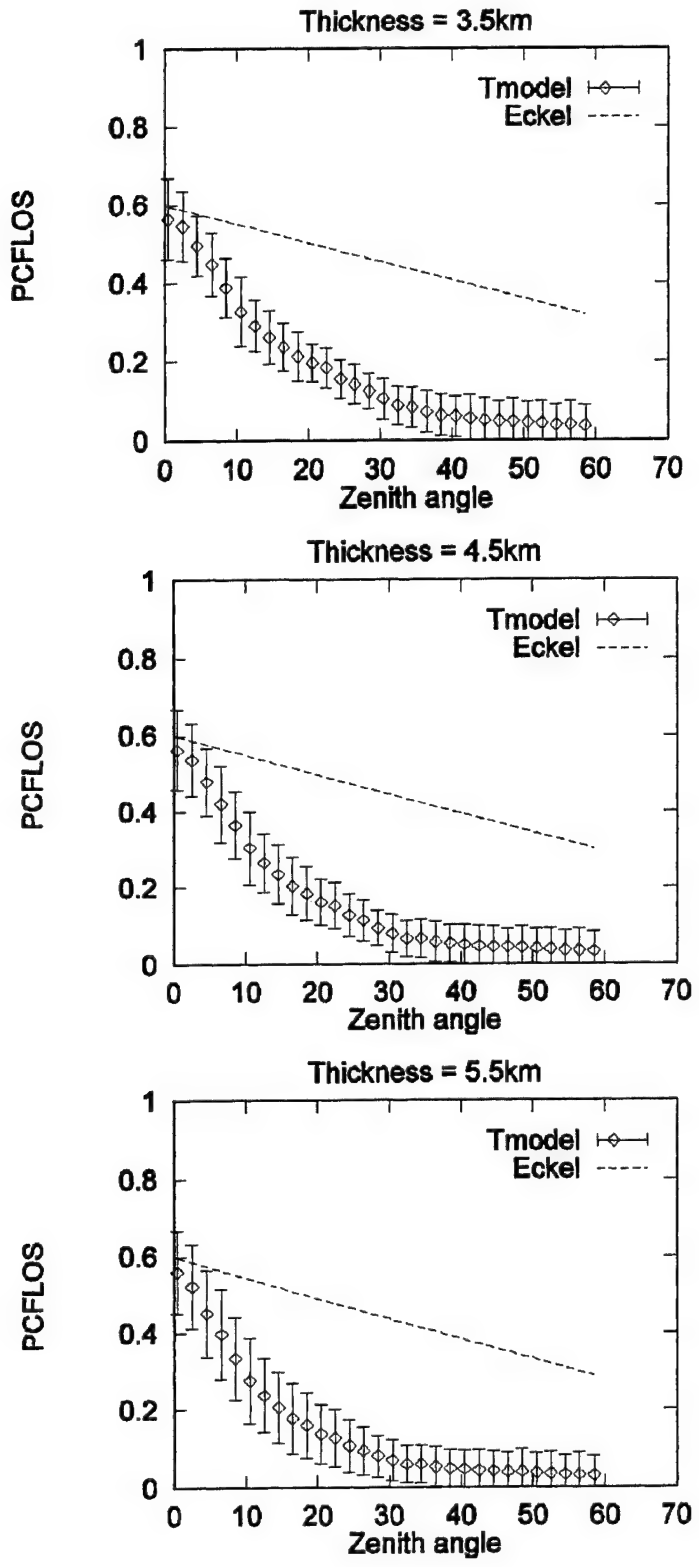

Figure 7. Tmodel Results for 40 Percent Coverage of Moderately Thick Clouds.

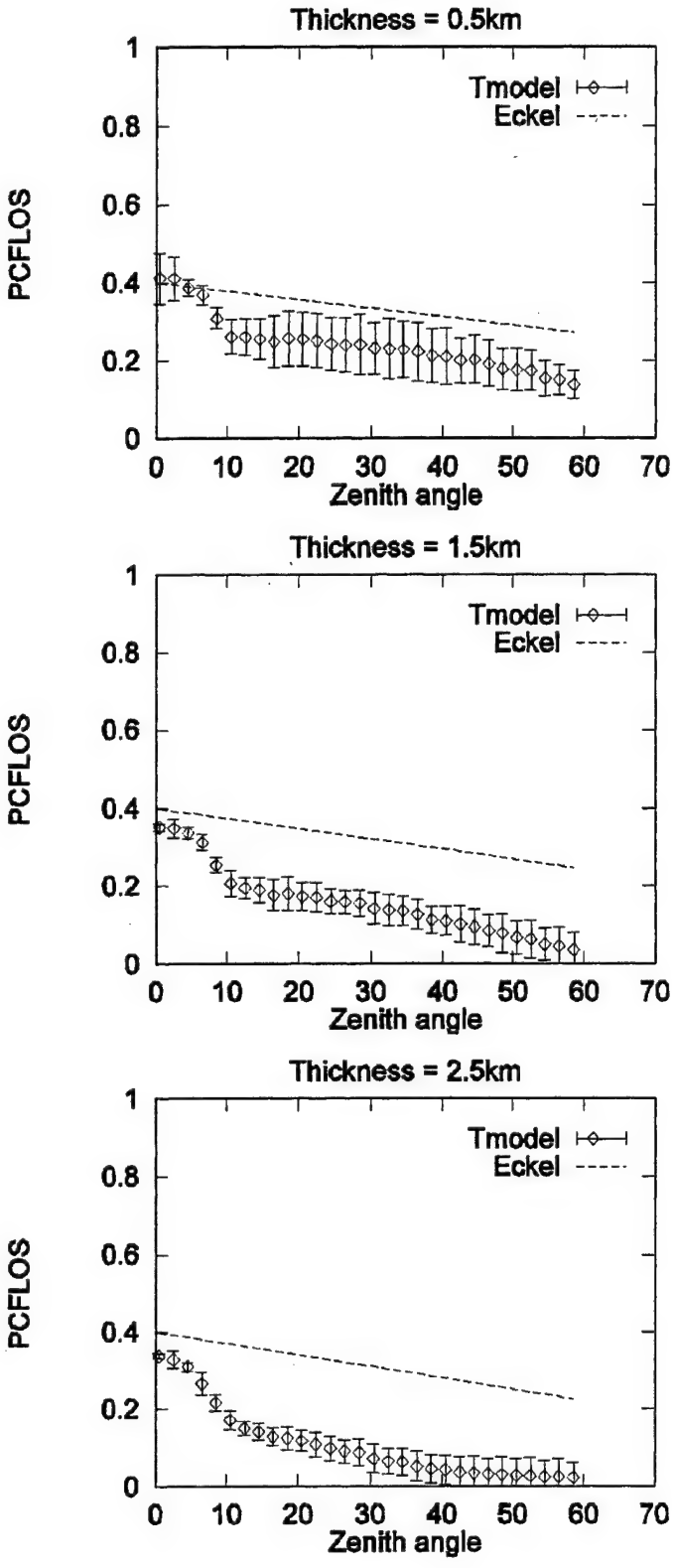

Figure 8. Tmodel Results for 60 Percent Coverage of Thin Clouds.

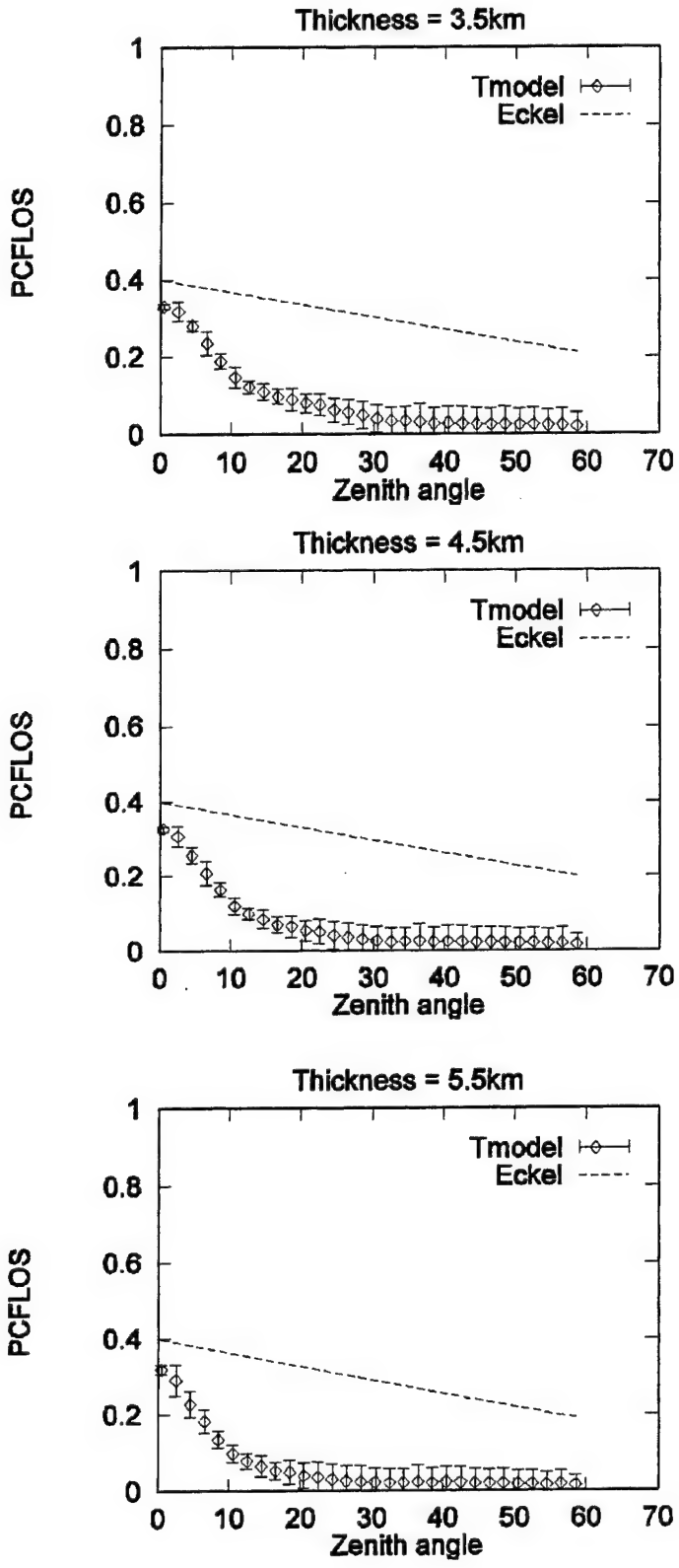

Figure 9. Tmodel Results for 60 Percent Coverage of Moderately Thick Clouds.

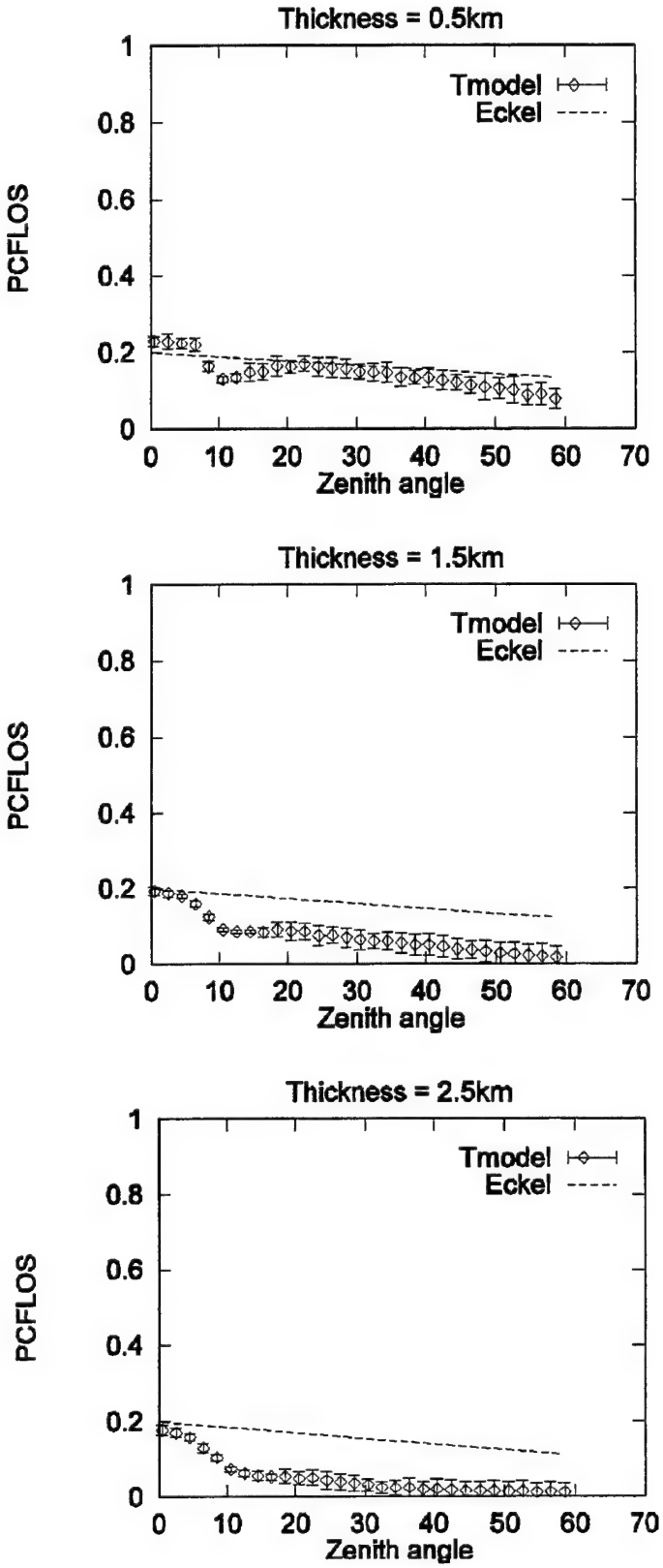

Figure 10. Tmodel Results for 80 Percent Coverage of Thin Clouds.

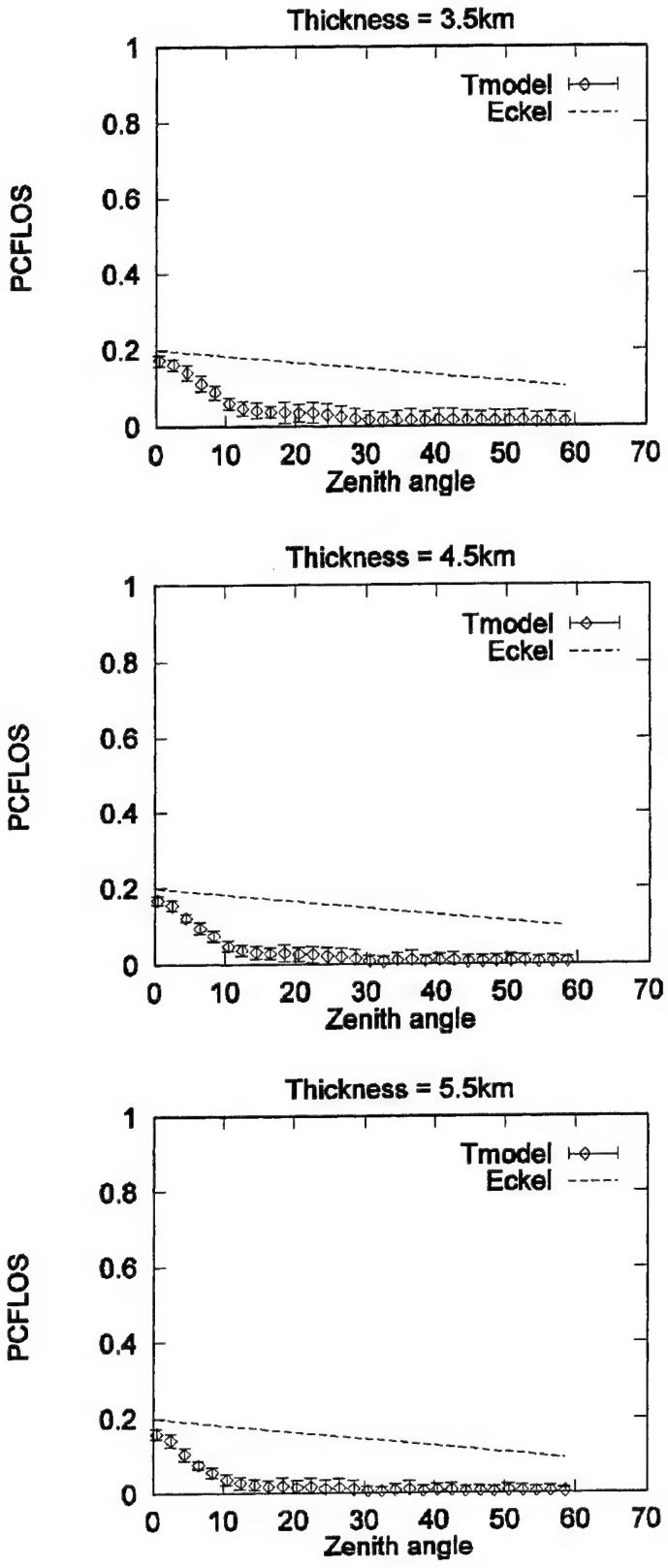

Figure 11. Tmodel Results for 80 Percent Coverage of Moderately Thick Clouds.

The average values represented in Figures 4 through 11 have been stored in a hypercube along with the additional PCFLOS values discussed that extend the range of the hypercube. The use of the hypercube is demonstrated by selecting a set of input values that requires interpolation in all three hypercube dimensions. Figure 12 shows PCFLOS values for a scene with 30 percent cloud coverage and 3.0 km thickness. The zenith angles are 1. 0°, 3.0°, ... 57.0° The figure shows PCFLOS values computed by hypercube interpolation along with values computed directly by tmodel. A comparison of these two curves shows that the hypercube produces acceptable results.

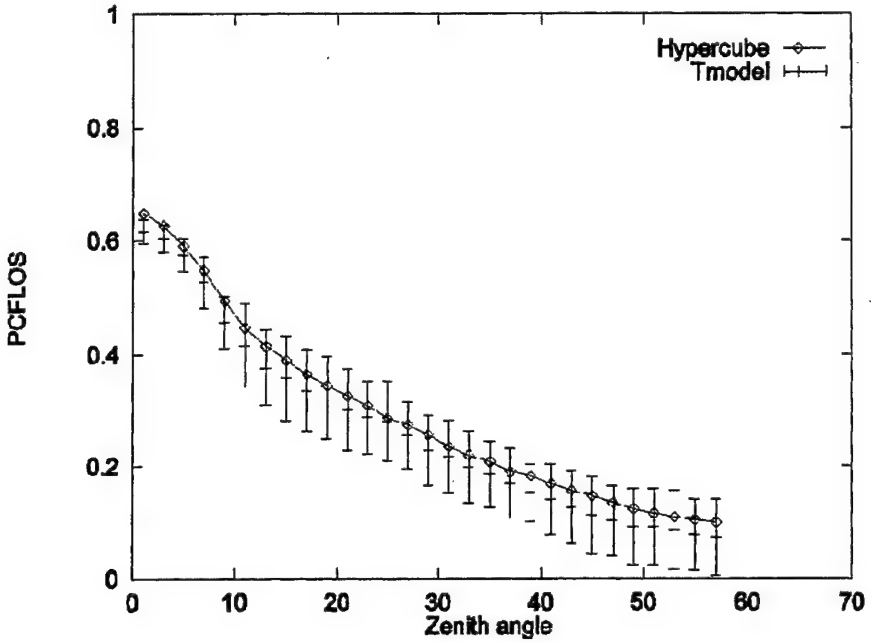

Figure 12. PCFLOS Values Due to Hypercube Interpolation and Direct Tmodel Calculation for 30 Percent Coverage, 3.0 km Thickness.

2.3 Model Improvements

Several improvements to the detailed model are made based on a review of the results shown in the previous section and further numerical experiments, including those done by [*Eckel and Crane*, 2000]. These improvements address problems associated with the tmodel geometry, the unrealistic effects of repeating like tiles, and the CSSM coverage errors. A limited number of test calculations is done with the improved model. Results are shown in this section.

Tmodel geometry is changed to meet the need of Eckel and Crane for results with missiles at a user-specified altitude that could be within the cloud deck. In the new arrangement the sensor is positioned relative to an origin that is in the middle of the missile field (rather than an origin on the

ground as was done originally). In addition to making the model more flexible with regard to missile altitude, this change improves the model's efficiency by reducing the number of tiles required at low zenith angles. In some cases this meant using only ten tiles, where previously dozens would have been required. Many calculations have been done with the new sensor geometry and no negative impacts of this change have been seen.

The practice of generating a clouded area by repeatedly copying a single cloud scene can lead to unrealistic effects, as shown in [*Eckel and Crane*, 2000]. For example, if the scene contains a cloud-free strip, then tiling copies can place these strips end-to-end, producing a long, cloud-free strip that extends through all the tiles. This allows a significant number of missiles to be seen at all zenith angles and is unlikely to occur in nature. This problem is solved by tiling several different scenes so that unusual cloud features do not have any undue influence on the outcome.

A large number of calculations has been done using the new sensor geometry along with the tile variation. Many of the calculations involved missiles within or above the clouds. Figure 13 shows PCFLOS results for four different missile altitudes for the same set of cloud tiles. The clouds are 1.0 km thick altocumulus clouds at a base of 1.0km and a coverage of 40 Percent. When the missiles are placed above the clouds, all missiles are detected as expected. As the missiles are lowered, so is the PCFLOS, though not in a linear fashion.

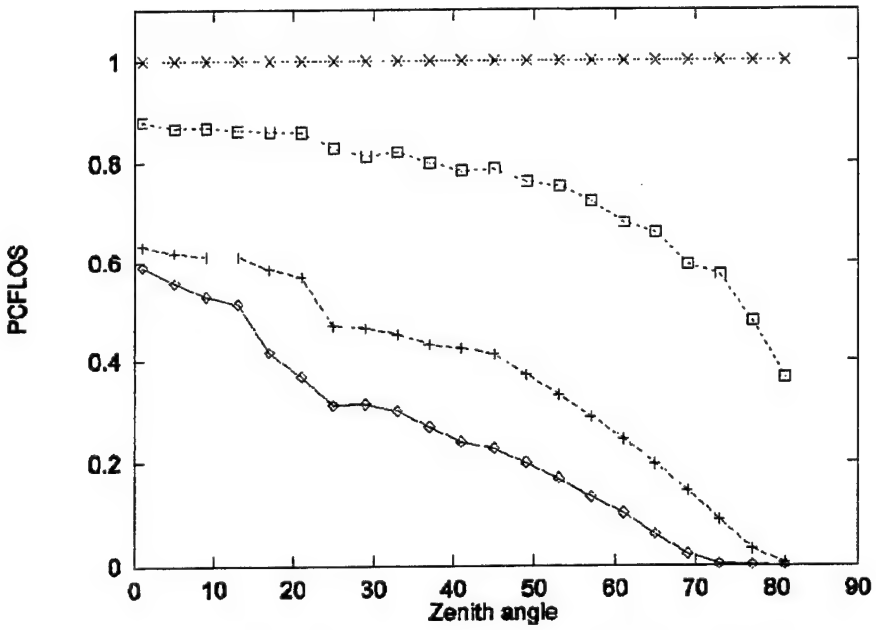

Figure 13. PCFLOS Values for Missiles at Various Altitudes.

As mentioned in Section 2.2, the CSSM produces coverage errors. When the results of four scenes are combined, the resulting error can be as large as 20 Percent. A correction can be made using quadratic interpolation. Consider PCFLOS as a function of coverage, with PCFLOS(0)=1 and PCFLOS(1)=0 (for any zenith angle). A third value, PCFLOS(C_a), where C_a is the actual coverage, comes from the detailed model and is the value being ``corrected." The actual coverage

is assumed to be one minus the PCFLOS for a zero zenith angle. The quadratic function through the three known PCFLOS values is

$$PCFLOS(C) = \left(\frac{1-C}{C_a}\right)\left(C_a - C + \frac{C \times PCFLOS(C_a)}{1-C_a}\right). \quad (1)$$

This function can be used to find PCFLOS at the desired coverage, C, and other conditions (zenith angle, cloud thickness, etc.) the same as for PCFLOS (C_a). A problem with this approach is that the function can produce negative PCFLOS values. This has been handled by setting negative PCFLOS values to zero.

Results of using Equation (1) with PCFLOS values represented in Figures 5 and 9 are shown in Figures 14 and 15, respectively. Each corrected value in these figures is found by applying Equation (1) to the PCFLOS value associated with each random number seed and then averaging those four results. The uncorrected values are the same as those shown in Figures 5 and 9 and are repeated here for reference. Figures 14 and 15 do not reflect the changes in tmodel geometry and tile variation discussed above.

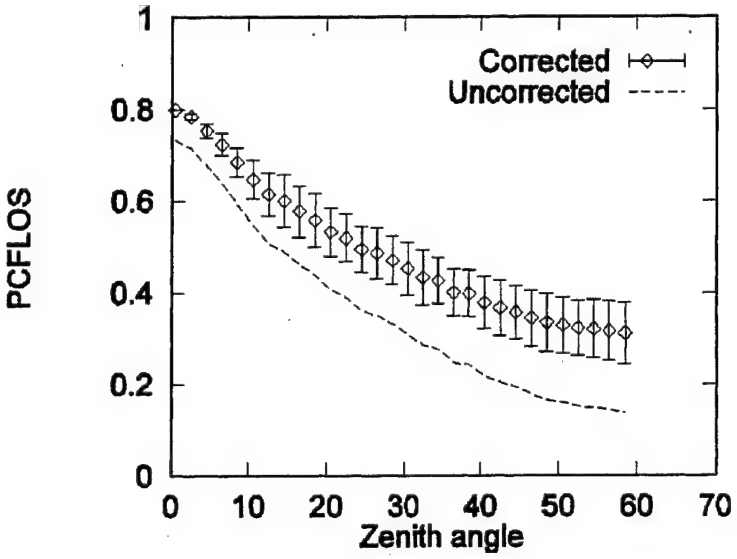

Figure 14. Coverage Corrected Tmodel Results for 20 Percent Coverage, 3.5 km Thickness.

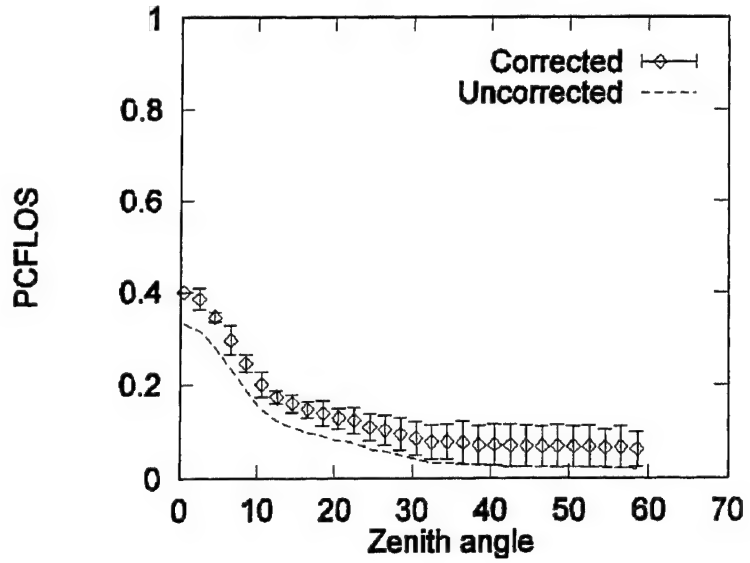

Figure 15. Coverage Corrected Tmodel Results for 60 Percent Coverage, 3.5 km Thickness.

3. VISIBLE AREA MODEL

The detailed model can provide the PCFLOS values needed but at a high computational cost. Therefore a fast alternative is explored. Since evaluating lines-of-sight is a geometric problem, a simplified approach is taken based on geometry and visible area. In this way, the fast approach has a physical basis. The next section contains a detailed discussion of the geometry of cloud interference, since this is not only the basis of the simplified model, but it is also useful in understanding detailed model results. Subsequent sections discuss the real-cloud considerations, the proposed model, and its results.

3.1 Geometry of Cloud Interference

If the shapes, sizes, and locations of clouds were known, then geometry could be used to compute, at least approximately, the fraction of area visible for a given zenith angle. The visible area can be taken as PCFLOS. Here we apply this idea to a fictitious cloud scenario. The calculation is done on a two-dimensional environment containing rectangular clouds.

Consider the gap between two rectangular clouds shown in Figure 16. On the left side of the gap is a cloud with its base at *(bx, by)* and on the right side of the gap is the top of another cloud at (*tx,ty*). When viewed from above with a zenith angle of 0° the visible area between the clouds is *tx* - *bx*. When viewed from a zenith angle of $\theta > 0°$, as shown in Figure 16, the right hand cloud blocks a region measuring $T \tan \theta$, where T is the effective thickness, *ty* - *by*, of the cloud. When part of the gap is blocked, the visible area between the clouds is reduced to

$$\text{visible area} = tx - bx - T \tan\theta. \tag{2}$$

As θ increases, the blocked region occupies more of the gap and visibility decreases. When

$$\theta > \tan^{-1}\left(\frac{tx - bx}{T}\right) \tag{3}$$

the blocked region occupies the entire gap and the visibility between these clouds is zero.

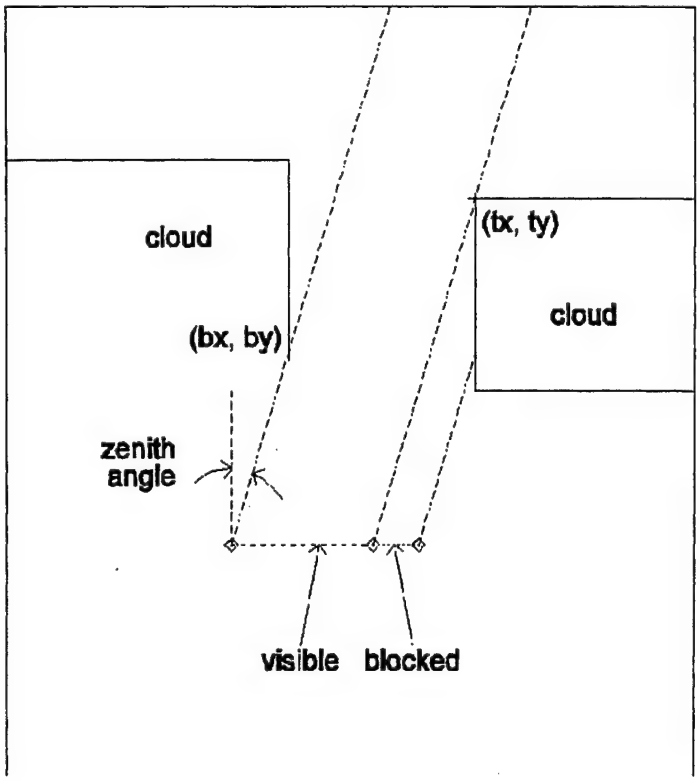

Figure 16. Visible and Blocked Areas for Rectangular Clouds.

A result of using rectangles to represent clouds is that the most favorable zenith angle (for maximum visible area) is 0°. It is recognized that in a given real environment the most favorable zenith angle may not be 0°. Consider the alternate cloud representation and the associated best zenith angle shown in Figure 17. For real-cloud scenarios that look more like Figure 17 than like rectangular clouds, the most favorable zenith angle is significantly greater than 0°. The model proposed here does not attempt to capture such specifics of a given real scenario. Instead the model uses rectangular clouds as a simple representation of an average of likely scenarios.

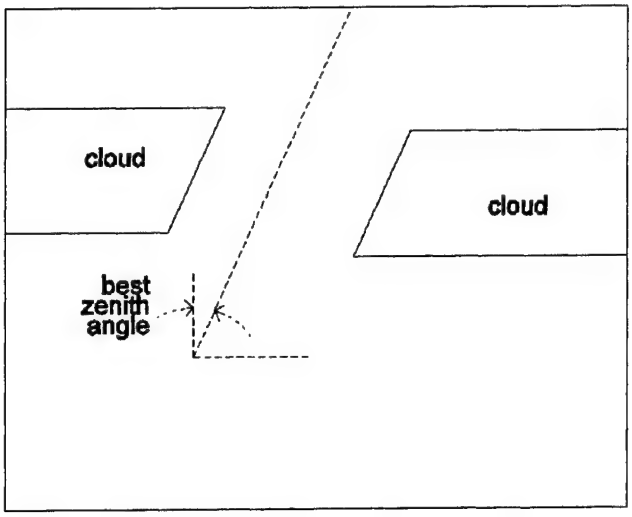

Figure 17. Optimal Zenith Angle for an Alternate Cloud Representation.

Notice that the altitudes *ty* and *by* only impact the result through the calculation of *T*, the effective thickness. If the clouds were shifted together vertically, the outcome would be the same. Similarly, if the altitude-of-interest, or missile altitude, is changed, but kept below *by*, the outcome would be the same. For an altitude-of-interest, *A*, that is within the clouds, the effective thickness would be *ty* - *A*. If $A > ty$, then the clouds do not interfere with the visibility for any zenith angle.

This kind of calculation can be done easily for any arrangement of rectangular clouds. Equations (2) and (3) are applied to each gap and the visible areas for all gaps are summed. Several cloud scenarios are considered to illustrate results for various cases. Periodic boundary conditions are used. In other words, the regions adjacent to the domain contain copies of the cloud arrangement that is inside the domain. In all cases, the altitude-of-interest is below the cloud base and so it is not specified.

Several cloud scenes are considered to illustrate the effects of varying cloud width and cloud thickness. A visibility calculation is done for the cloud scene shown in Figure 18. Even though there is only one cloud inside the domain, it forms a gap together with the (identical) cloud in the adjacent domain, due to the periodic boundary condition. The fraction of cloud coverage, *C*, is 0.50, the average thickness is about 2.0 km, and the cloud coverage is contained in a single cloud. The fraction of visible area for a range of zenith angles is shown in Figure 19. When the zenith angle is above about 86°, the domain is completely blocked and the visible area is zero.

Another cloud scene with $C = 0.5$ and $T \approx 2.0$ is shown in Figure 20. In this scene the cloud coverage is distributed over three clouds. The resulting fraction of visible area, shown in Figure 21, is lower for this case than for the single-cloud case (for zenith angles above 0°). This is because the cloud-free portion of the scene in Figure 20 is distributed over more gaps, each of which contains a blocked region. The faster drop-off in visibility here is due to the larger number of blocked regions (or gaps). Since the gaps in Figure 20 are smaller than those in Figure 18, they become completely blocked at a lower zenith angle.

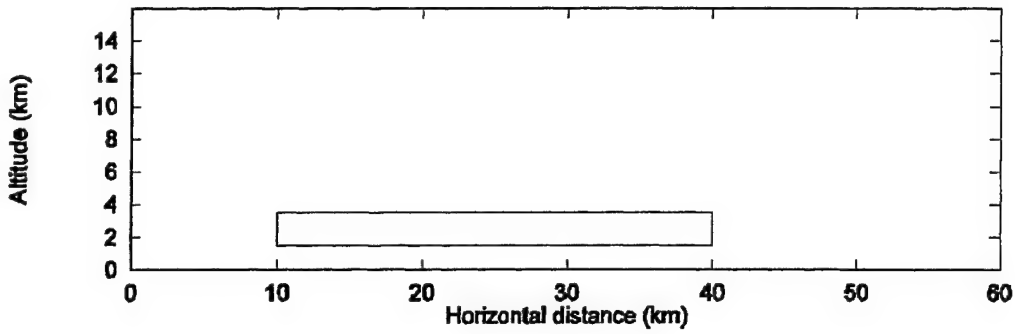

Figure 18. Scene With One Cloud and $C = 0.5$, $T \approx 2.0$.

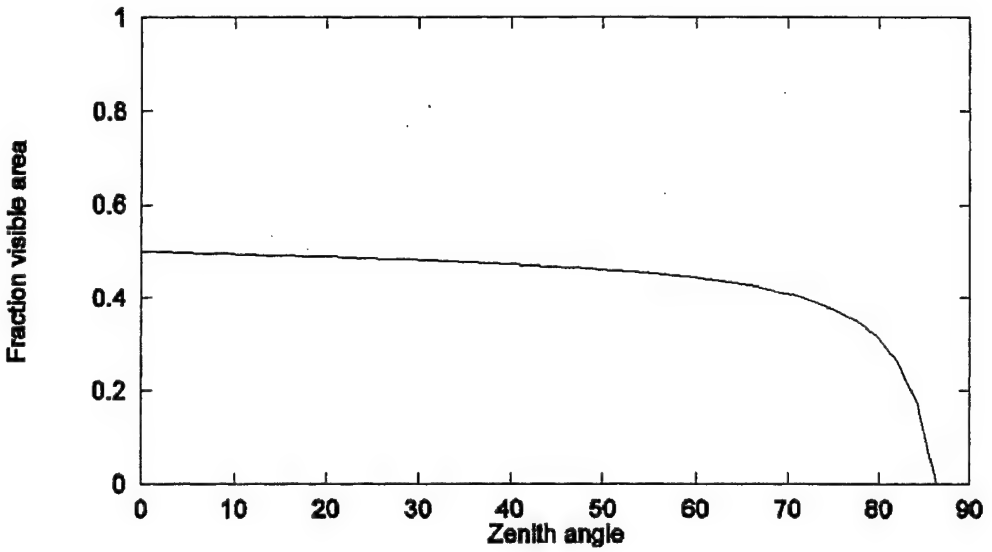

Figure 19. Visible Area for Scene With One Cloud and $C = 0.5$, $T \approx 2.0$.

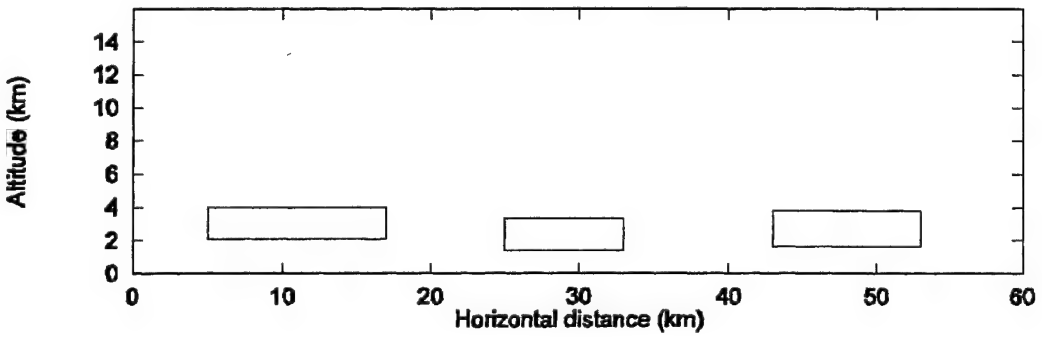

Figure 20. Scene With Three Clouds and $C = 0.5$, $T \approx 2.0$.

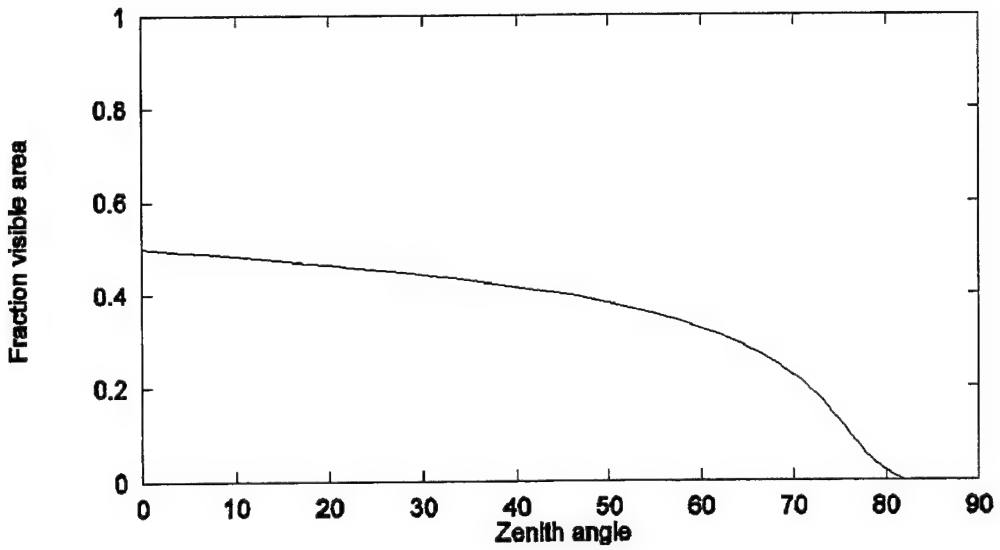

Figure 21. Visibility for Scene With Three Clouds and $C = 0.5$, $T \approx 2.0$.

The effect of cloud thickness is shown by maintaining the coverage at $C = 0.5$ and setting $T \approx 12.0$ as shown in Figure 22. The associated fraction of visible area, shown in Figure 23 is lower than for the similar cloud arrangement of thinner clouds (Figures 20 and 21).

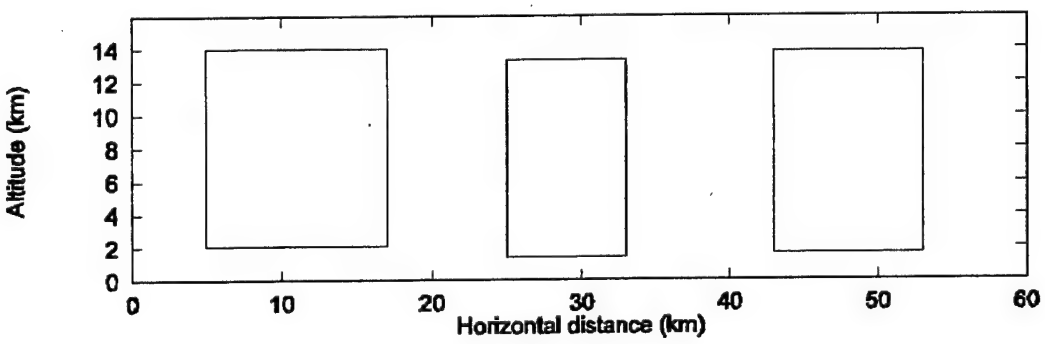

Figure 22. Scene With Three Clouds and $C = 0.5$, $T \approx 2.0$.

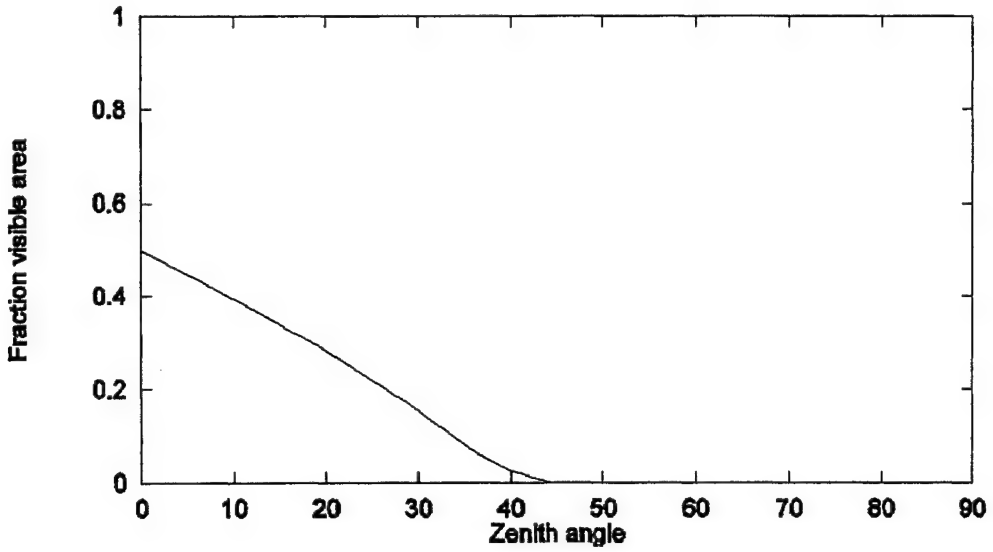

Figure 23. Visible Area for Scene With Three Clouds and $C = 0.5$, $T \approx 2.0$.

The visible area curves for the different cloud arrangements exhibit several features that might be expected based on intuition and on inspection of Equations (2) and (3). For example, increasing the number of clouds, while keeping the coverage and other variables fixed, results in a decrease in visible area for zenith angles above 0°. To see how Equations (2) and (3) lead to this result notice that for each gap the visible area is reduced by up to $T \tan \theta$. This corresponds to the blocked region for each gap. Since more clouds means more gaps and more blocked regions, it also means reduced visible area. When cloud thickness increases, visible area for zenith angles above 0° decreases. This makes sense intuitively and it is clear from inspection of Equation (2) that increasing T decreases visible area.

A feature of all of the examples presented is that when the zenith angle is large enough all lines-of-sight are blocked by clouds. This is a shortcoming of the two-dimensional assumption. The three-dimensional environment might actually contain one two-dimensional slice that is heavily clouded and another slice that is nearly cloud-free. In the nearly cloud-free slice a CFLOS would be possible even for very high zenith angles. Since the visibility for the three-dimensional environment would take into account all slices, it would allow some chance of a CFLOS for very high zenith angles, while a single two-dimensional slice that contains clouds does not. This shortcoming of the two-dimensional assumption can be mitigated by considering several two-dimensional cloud scenarios and combining the results. This may be viewed as using several different two-dimensional slices of a three-dimensional cloud scenario to represent the entire space. This is discussed further in Section 3.3.

The approach taken here requires specific cloud scenarios. This may be considered a drawback because it adds a step to the visible area calculation. The additional step can be made worthwhile, however, when it is used to incorporate meteorological considerations. These are discussed in Section 3.2.

3.2 Real-Cloud Considerations

The cloud arrangements used with the visible area model must be constructed under consideration of cloud scenes occurring in nature. This section reviews the relevant cloud observations.

As shown in the previous section, it is the shapes of the gaps between clouds that are important for the geometry-based approach. While gap thickness is known, gap width must be approximated. Equivalently, cloud width can be approximated, since gap dimensions follow from cloud dimensions (and percent cloud coverage). Cloud observations reported in [*Byer*, 1944], [*WMO*, 1969], and [*Kessler*, 1986] are used to determine appropriate widths.

For the purposes of generalizing cloud dimensions, clouds are grouped according to three altitude categories: high, middle, and low. In addition, cloud thickness is considered to distinguish two cloud types in the low-altitude cloud group. Finer distinctions between clouds are judged infeasible due to the constraints imposed by the limited input (base, thickness, altitude, and coverage) and the need for speed and simplicity. It is recognized that the four cloud types used here each contain a great variety of clouds that can have a broad range of widths. Many specific values are discussed in this section and serve as guidelines for cloud width ranges used by the visible area model.

High-altitude clouds, which include cirrus, cirrocumulus, and cirrostratus, are those with base altitudes greater than 6 km. The typical width of a cirrus cloud is 1.5 km or more while that of a cirrocumulus cloud is only about 0.1 km.

Low-altitude clouds, or clouds with base altitudes below 2 km, are cumulonimbus, cumulus, stratocumulus, stratus, and nimbostratus. These clouds can be divided into two groups based on thickness: cumulonimbus and others. Cumulonimbus clouds are very thick, typically thicker than 12.0 km, and tend to be 2.5 km to 8.0 km wide. The remainder of the low-altitude clouds are thinner and, on average, are smaller in width. For example, stratocumulus clouds, which occur as rolls, with or without breaks, tend to be less than 0.5 km in width, while cumulus clouds can be much wider than this.

Middle-level clouds occur with base altitudes between 2 and 6 km and include altocumulus and altostratus. Altocumulus clouds, which are small relative to other clouds found at middle levels, are typically 0.25 to 0.5 km in width.

3.3 Model Description

A PCFLOS based on geometry is calculated using the known cloud metrics and cloud widths, which are assigned in consideration of real-cloud observations. The calculation relies on several fictitious, homogeneous cloud scenarios, in which all clouds are assumed to be opaque to the weapon sensor. For each scenario one cloud width is assigned. Together, the scenarios represent a range of appropriate cloud widths. The visible area for each scenario is calculated following the ideas of Section 3.1. An additional scenario gives visible area in the case of a cloud front, or a cloud resembling an unbroken sheet. The results of the different scenarios are combined to give the final PCFLOS. The calculation is explained in this section and summarized in the Appendix.

The model determines minimum and maximum cloud widths based on cloud type. Since real-cloud considerations do not provide definitive cloud-width ranges, the parameters used to compute the minimum and maximum cloud widths are subject to tuning for agreement with the detailed model.

The model uses three functions to identify which of the cloud types are applicable based on cloud thickness[1], T, and the altitude of the cloud base, B. For example, if B is near the threshold between middle-level clouds and high clouds, then the functions identify both middle and high cloud types and assign weights to each type. These functions are smooth approximations of the step functions that would be implied by assigning only one cloud type to each T, B pair. Function values are used in a summation to switch on or off terms associated with each cloud type.

The function b_l identifies the clouds with low-altitude bases. It is given by

$$b_l \equiv \frac{1+\tanh[\beta_l(B-B_l)]}{2} \tag{4}$$

and has a value near one when the cloud base is below the low-altitude threshold, B_l. Otherwise b_l is near zero. The value of β_l determines how quickly the function changes near $B = B_l$. The function b_h, given by

$$b_h = \frac{1+\tanh[\beta_h(B-B_h)]}{2} \tag{5}$$

is near one for high-altitude bases, or when $B > B_h$, where B_h is the high-altitude threshold. For $B < B_h$, this function is near zero. Therefore, low clouds have $b_l \approx 1$, $b_h \approx 0$, middle-level clouds have $b_l \approx 0$, $b_h \approx 0$, and high clouds have $b_l \approx 0$, $b_h \approx 1$. With B given in km, appropriate values for the parameters in Equations 4 and 5 are $B_l = 2.0$, $B_h = 6.0$ and $\beta_l = \beta_h = 4.0$.

A third cloud-typing function, which is based on thickness, is given by

$$t_g = \frac{1+\tanh[\tau(T-T_g)]}{2} \tag{6}$$

Its value is near one for $T > T_g$. The parameter, τ, determines how quickly the function changes near the threshold T_g. For thickness T given in km the values $T_g = 8.0$ and $\tau = 8.0$ are used.

The functions b_l, b_h, and t_g are used to calculate w^0 and w^1, minimum and maximum cloud widths, respectively. The idea behind the w^0 calculation is to increment a fixed value representing middle-level clouds, m^0, by adjustments, Δ_h^0, Δ_l^0, and Δ_t^0, that are appropriate for clouds that are high, low, or thick, respectively. The values of these parameters are subject to tuning. The width w^0 is calculated as

[1] Note T is the total cloud thickness and it should not be changed when the altitude of interest (missile altitude) is higher than the cloud base. This situation is addressed later in this section.

$$w^0 = m^0 + b_h\Delta_h^0 + b_l(\Delta_l^0 + t_g\Delta_t^0). \tag{7}$$

The maximum cloud width is found similarly using

$$w^1 = m^1 + b_h\Delta_h^1 + b_l(\Delta_l^1 + t_g\Delta_t^1). \tag{8}$$

where the parameters m^1, Δ_h^1, Δ_l^1, and Δ_t^1 are to be determined through tuning.

The two values w^0 and w^1 are used as bounds for typical cloud widths, W_1, W_2, ..., W_n. Setting n=4 is appropriate since greater values of n are not found to significantly change the outcome and require more computation. For simplicity, the typical widths are assigned according to

$$W_i = w^0 + \frac{i-1}{n-1}(w^1 - w^0),\ i = 1, ..., n \tag{9}$$

so that $W_1 = w^0$ and $W_n = w^1$.

Once the cloud widths are assigned the fraction of visible area can be calculated for each one. The calculation assumes that the clouds are uniform and evenly spaced (so base, thickness, cloud width, and gap width are the same for all clouds in the scene). Numerical experimentation with the proposed model shows that uniform scenarios and scenarios with small, but significant variations lead to similar results. Therefore, the simpler, uniform scenario is assumed. If the altitude of interest is higher than the cloud base, then the cloud thickness above this altitude, $\tilde{T}$, is used for the visibility calculation. Otherwise $\tilde{T}$ is simply set equal to T. First, the zenith angle above which the entire domain is blocked is found for each width as

$$\theta_i^* = \tan^{-1}\left(\frac{W_i(1-C)}{\tilde{T}C}\right) \tag{10}$$

for $i = 1, ..., n$. Then the fraction of visible area for each width is given by

$$v_i = \begin{cases} 1 - C(1 + \dfrac{\tilde{T}}{W_i}\tan\theta), & \theta < \theta_i^*, \\ 0, & \theta > \theta_i^*, \end{cases} \tag{11}$$

for $i = 1, ..., n$ and $0° \le \theta < 90°$. The results reflect the fraction of area that is visible for each two-dimensional slice.

The visibility in the presence of a cloud front, or single sheet-like cloud, is also calculated. If two-dimensional slices are taken perpendicular to a cloud front, as shown in Figure 24, then the situation is equivalent to those described above. That is, once the cloud width is assigned, the calculation is carried out according to Equations (10) and (11) to obtain θ_{n+1}^* and v_{n+1}, respectively. The width for this calculation can be taken to be

$$W_{n+1} = C * L, \tag{12}$$

where L is the length of the domain in km. Recall that this calculation uses a periodic boundary condition so that the adjacent domain contains another cloud front of width W_{n+1}.

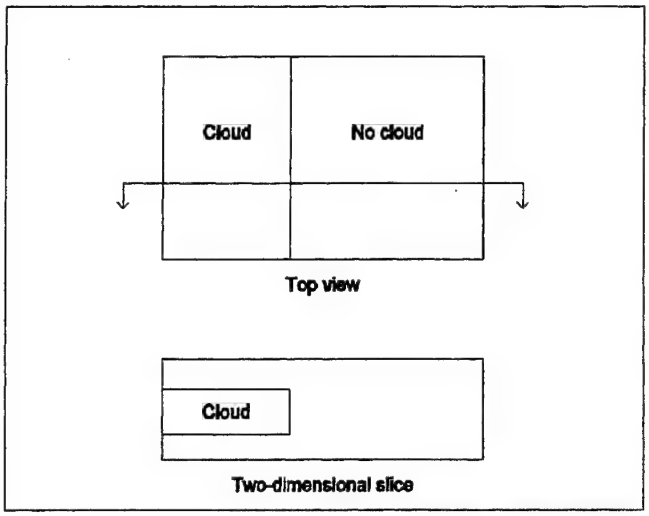

Figure 24. Top and Side Views of Cloud-Front Scene.

Consider slices taken parallel to a cloud front. One slice might be completely clouded while another is completely cloud-free. In either case the chance of a CFLOS does not vary with zenith angle. The fraction of visible area would be zero for slices through the clouded region and one for slices through the unclouded region. The chances of slicing through the clouded and unclouded regions are C and 1 - C, respectively. Combining the areas with the chances of slicing through the clouded and unclouded regions gives a PCFLOS of 1 - C for all look angles, assuming the LOS is parallel to the front. The two extreme orientations with respect to a front are combined with equal weight to give the visibility in the presence of a front as

$$v_f = \frac{1}{2}(v_{n+1} + 1 - C). \tag{13}$$

The visibility results produced by Equations (11) and (13) are combined to obtain PCFLOS. For simplicity, a linear combination is taken in which $v_1, \ldots v_n$ are given equal weight and v_f is weighted by p_f, the probability that the clouds occur in a front. The PCFLOS is given by

$$PCFLOS = p_f v_f + (1 - p_f)\frac{\sum_i v_i}{n} \tag{14}$$

To set p_f so that the probability of a front is equal to the probability of any of the other scenarios (or to give v_f and v_1 equal weight), the assignment $p_f = 1/(n+1)$ is made. This is a simple and reasonable choice when n=4.

3.4 Tuning and Results

The parameters involved in cloud-width assignment for the visible area model are evaluated through a tuning process. Parameters are initially assigned using only real-cloud observations and then adjusted to improve agreement between the visible area results and the detailed model results. Detailed model results are available for low clouds with small to moderate thicknesses. Thus, tuning is carried out for this limited group of clouds.

Values for m^0 and m^1 are needed to apply Equations (7) and (8). Since these parameters pertain to middle-level clouds, which are not of interest here, the values can be chosen arbitrarily. The assignments m^0=0.3 and m^1=4.0 are made with cloud considerations in mind and are held fixed during the tuning process. The initial parameter assignments, Δ_l^0=0.7, Δ_l^1=6.0, set the width range for low clouds to 1.0 - 10.0 km (or $m^0+\ \Delta_l^0\ -\ m^1+\ \Delta_l^1$). The other parameters referenced in the equations are not needed since they are multiplied by zero for low clouds with small to moderate thicknesses.

Examples of PCFLOS results due to the initial parameter settings are shown in Figures 25 through 26. The visible area curves are too high in comparison to the detailed model curves, also shown in the figures. This is typical among the cases considered for tuning purposes, which coincide with the tmodel cases used to populate the hypercube. The overestimation of PCFLOS can be improved by decreasing cloud width, which effectively increases the number of clouds and the amount of area blocked by clouds. After incremental adjustments and visual comparisons with detailed model results, the values Δ_l^0=0.6, Δ_l^1=1.75 are found to give good agreement. These parameter values imply a cloud-width range of 0.9 - 5.75 km for low clouds.

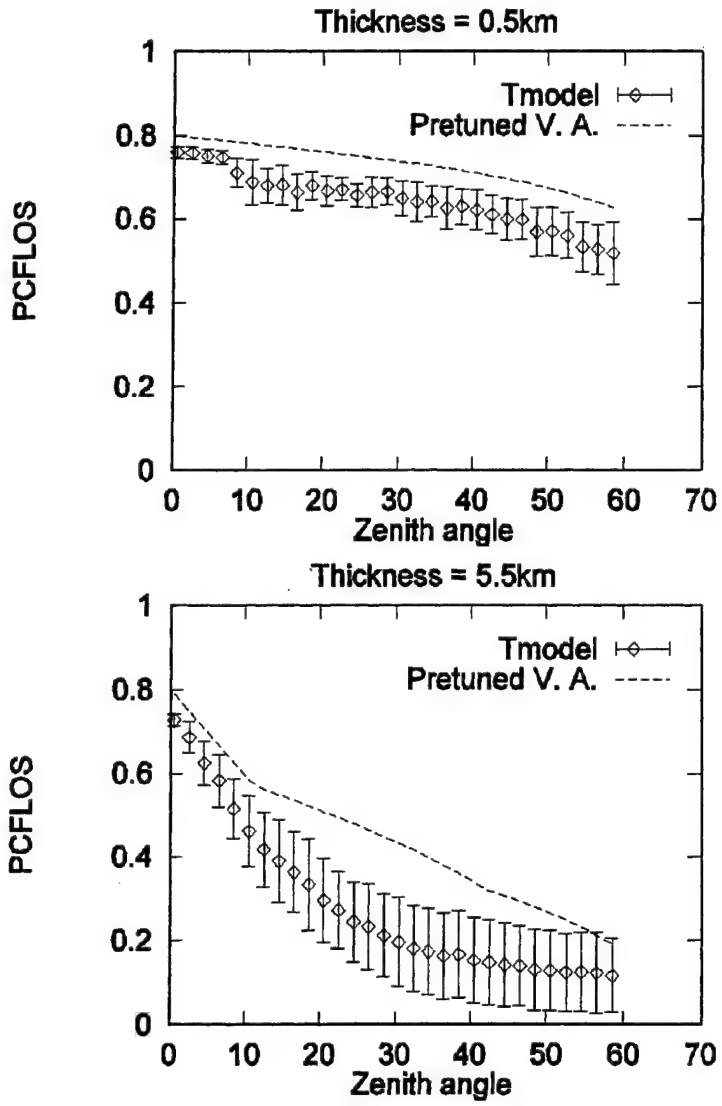

Figure 25. Results of Pretuned Visible Area Model and Detailed Model for 20 Percent Coverage.

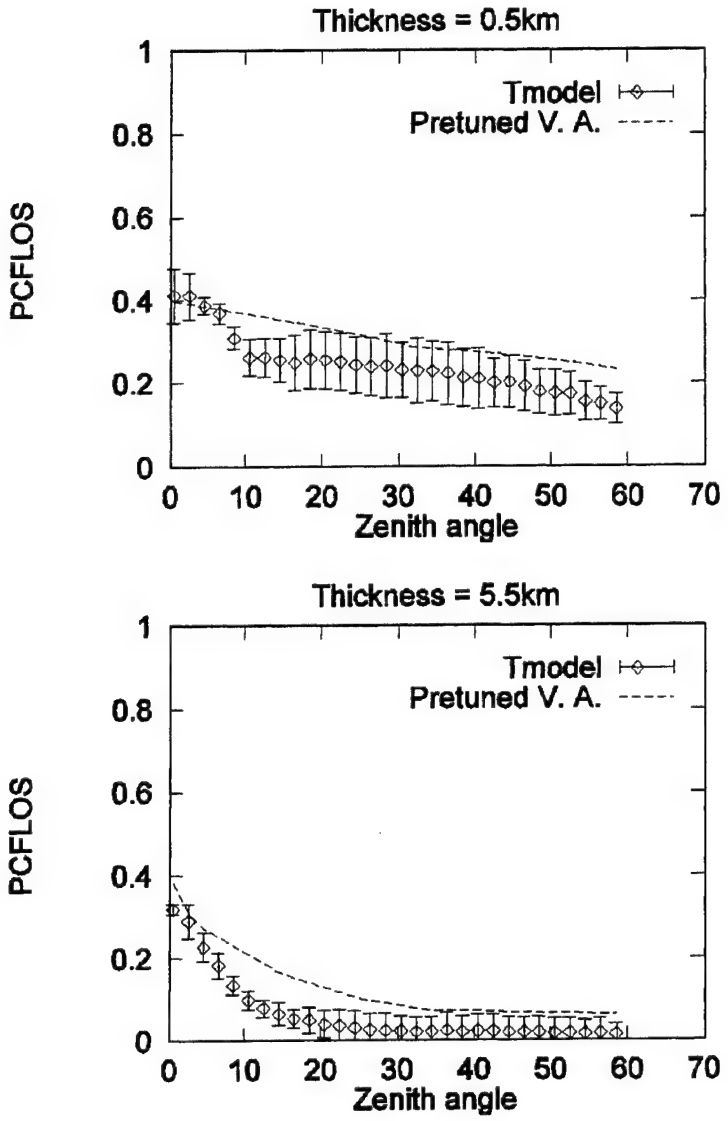

Figure 26. Results of Pretuned Visible Area Model and Detailed Model for 60 Percent Coverage.

Figures 27 through 34 show PCFLOS curves obtained with the final parameter values, along with tmodel results. The visible area model generally succeeds in capturing the rapid decrease in PCFLOS with increasing zenith angle that occurs for thicker clouds, according to the detailed model. An exception to this is seen for the highest coverage considered, 80 percent, where the visible area model predicts this decrease at a different zenith angle than the detailed model. On the other hand, the visible area model does not contain some of the undesirable artifacts seen in the detailed model results. For example, PCFLOS values predicted by the visible area model are 1 - C at a 0° zenith angle and monotonically decrease with increasing zenith angle.

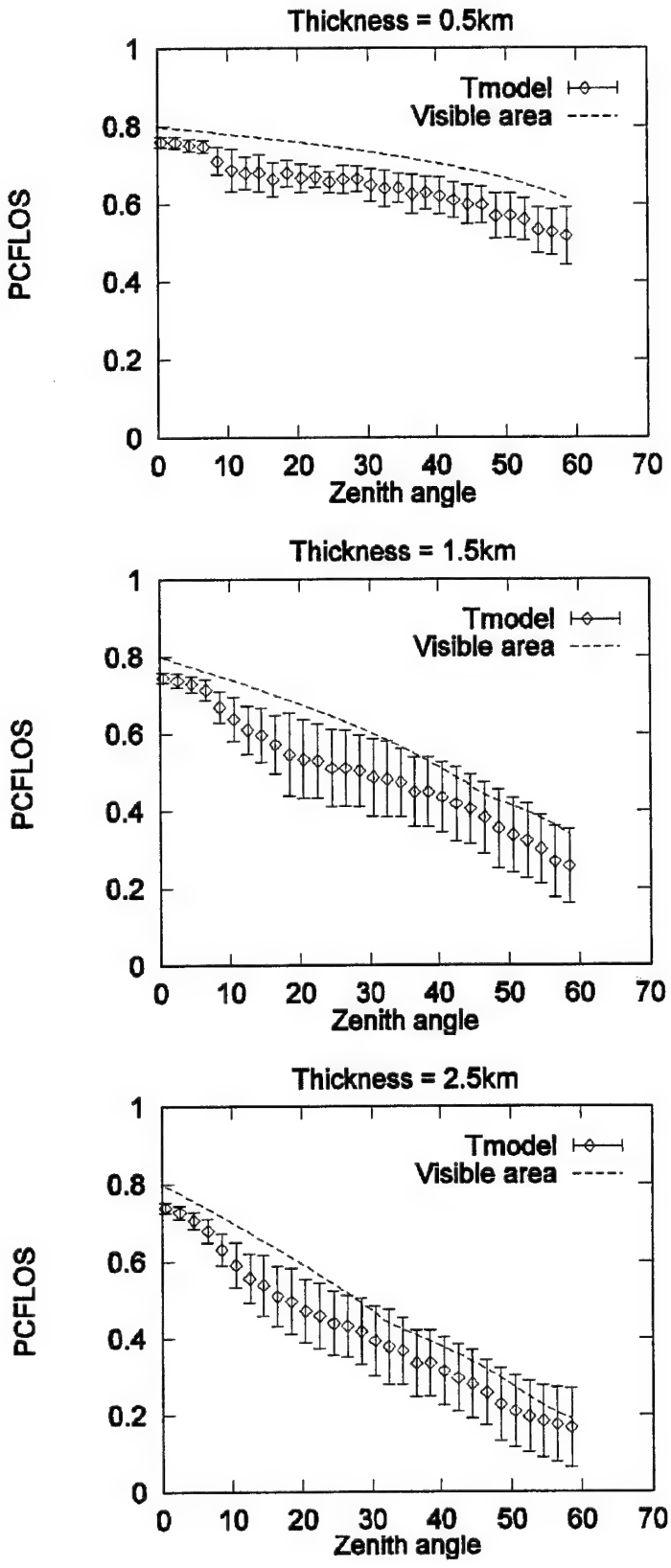

Figure 27. Visible Area Results for 20 Percent Coverage of Thin Clouds.

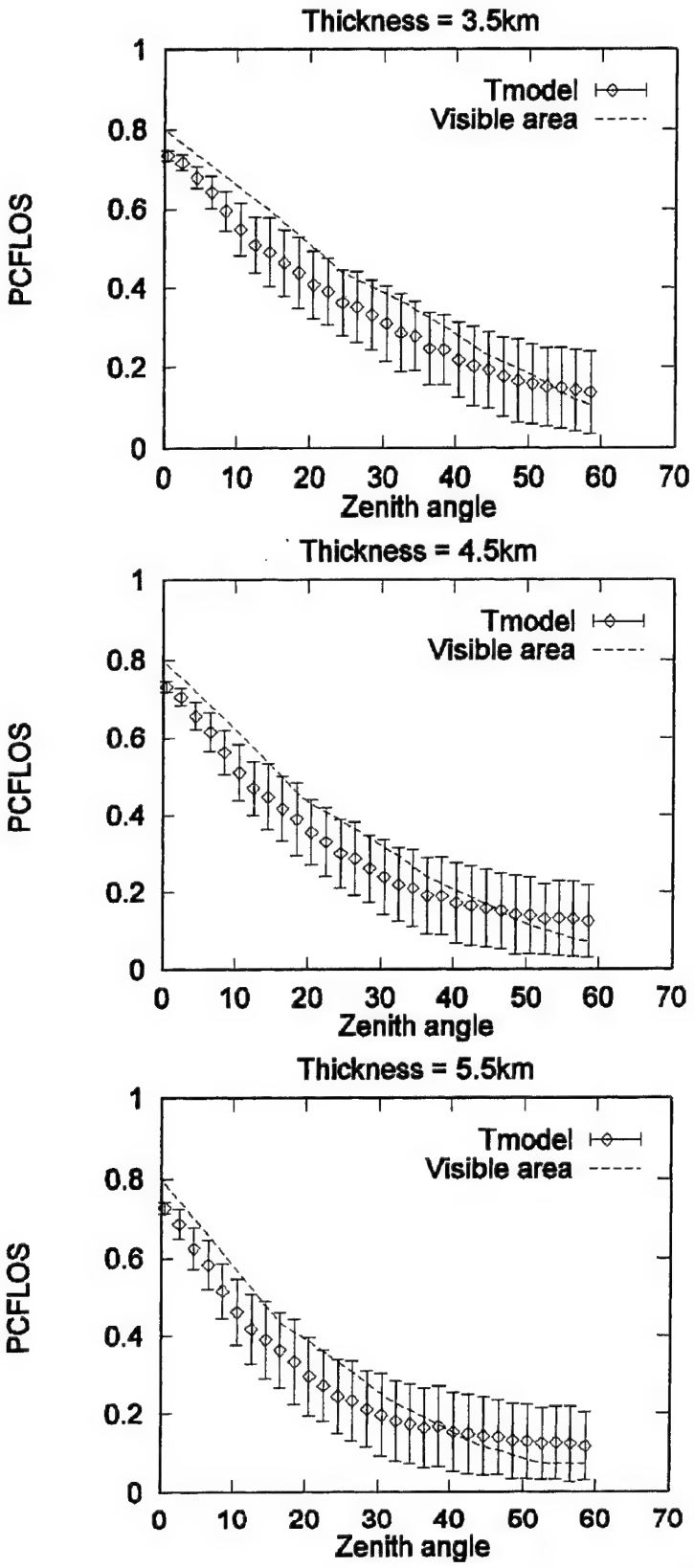

Figure 28. Visible Area Results for 20 Percent Coverage of Moderately Thick Clouds.

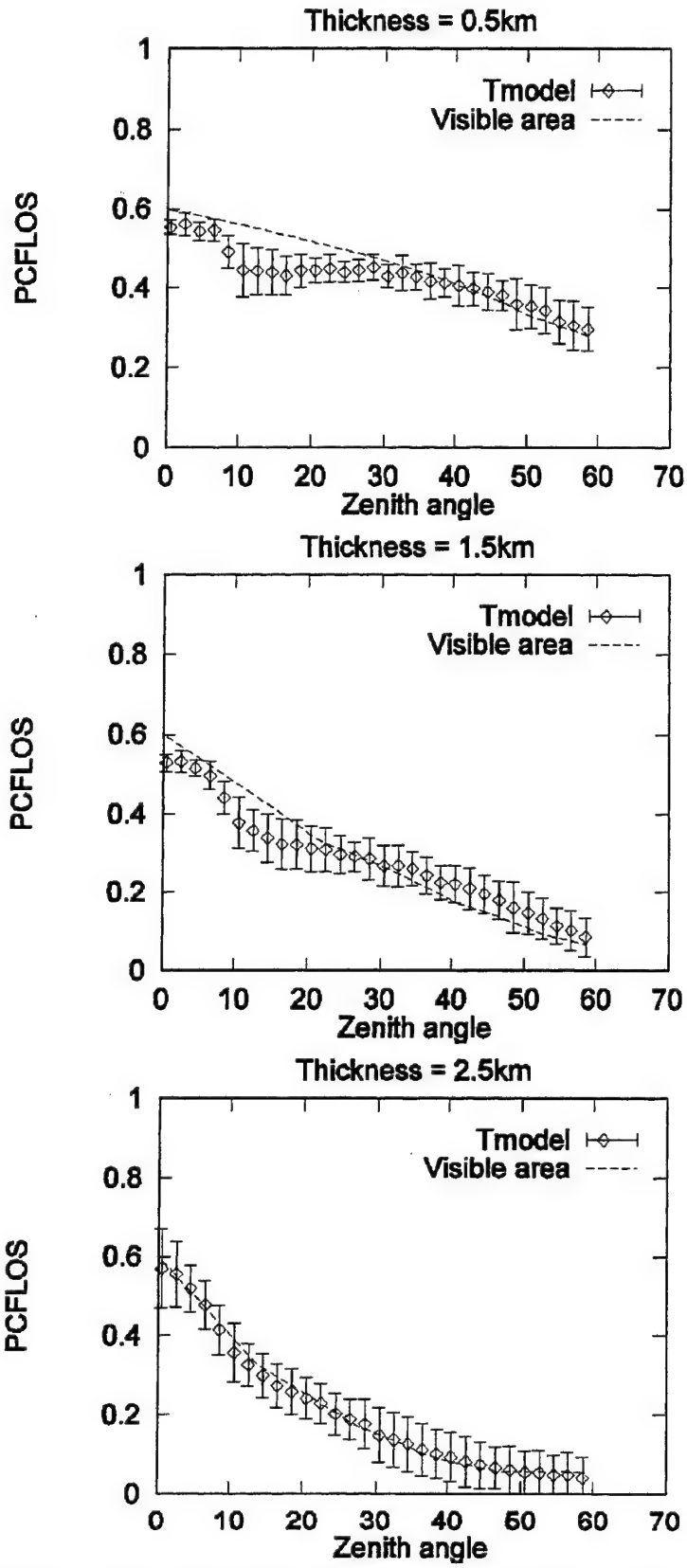

Figure 29. Visible Area Results for 40 Percent Coverage of Thin Clouds.

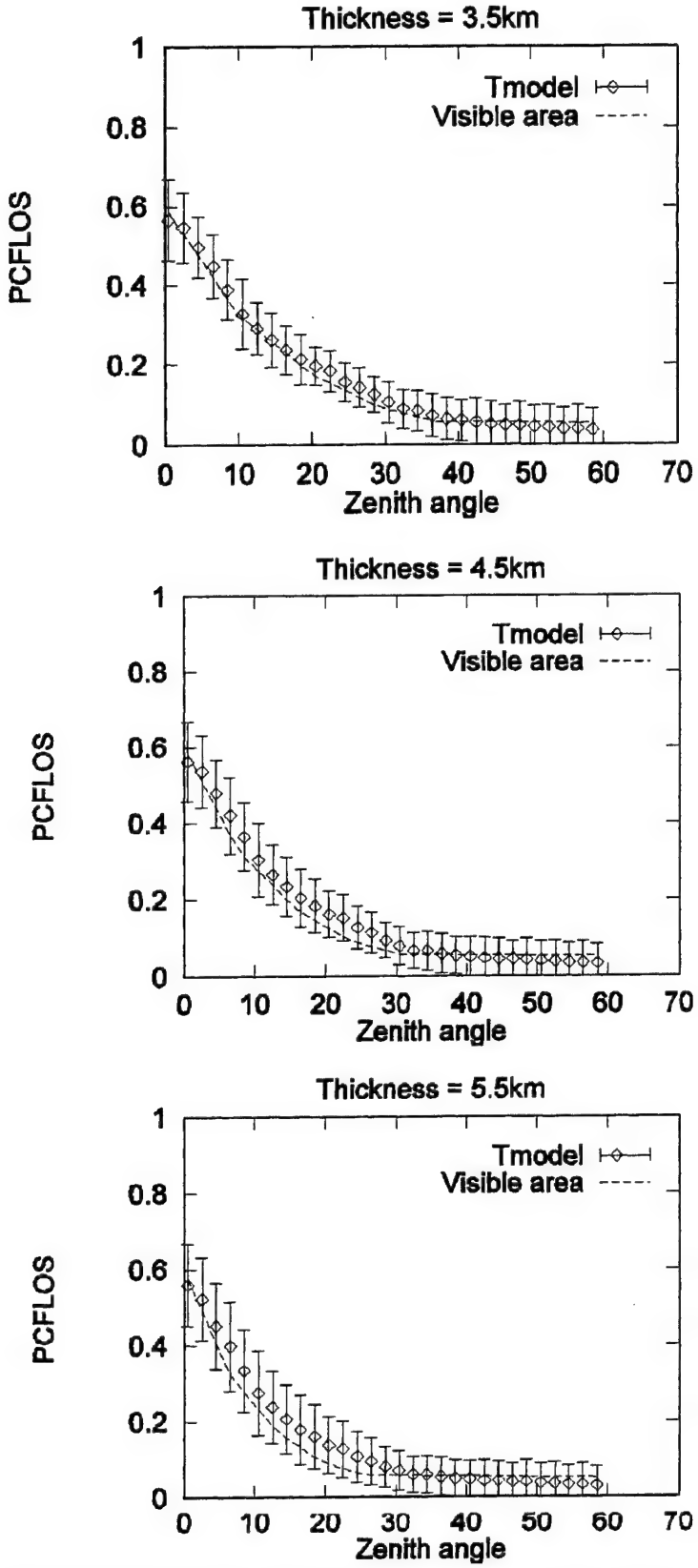

Figure 30. Visible Area Results for 40 Percent Coverage of Moderately Thick Clouds.

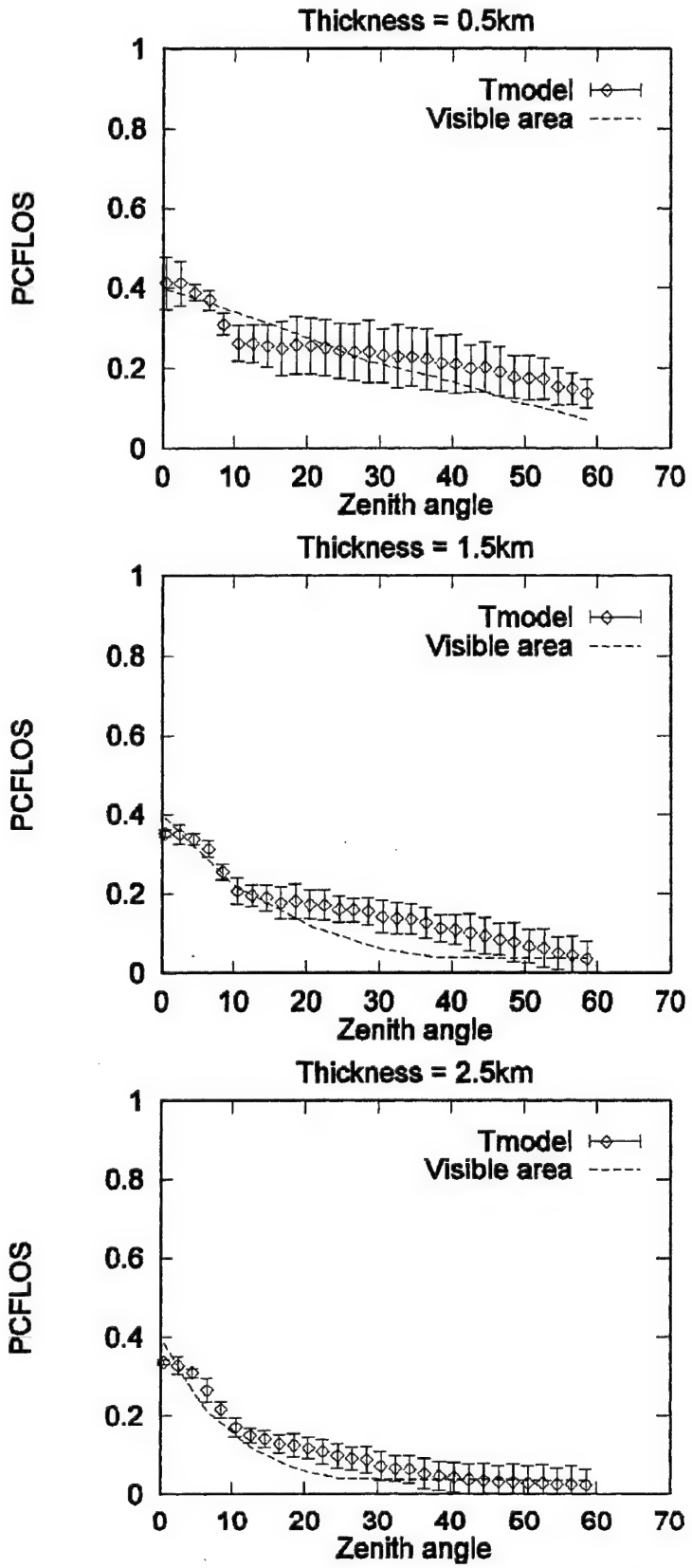

Figure 31. Visible Area Results for 60 Percent Coverage of Thin Clouds.

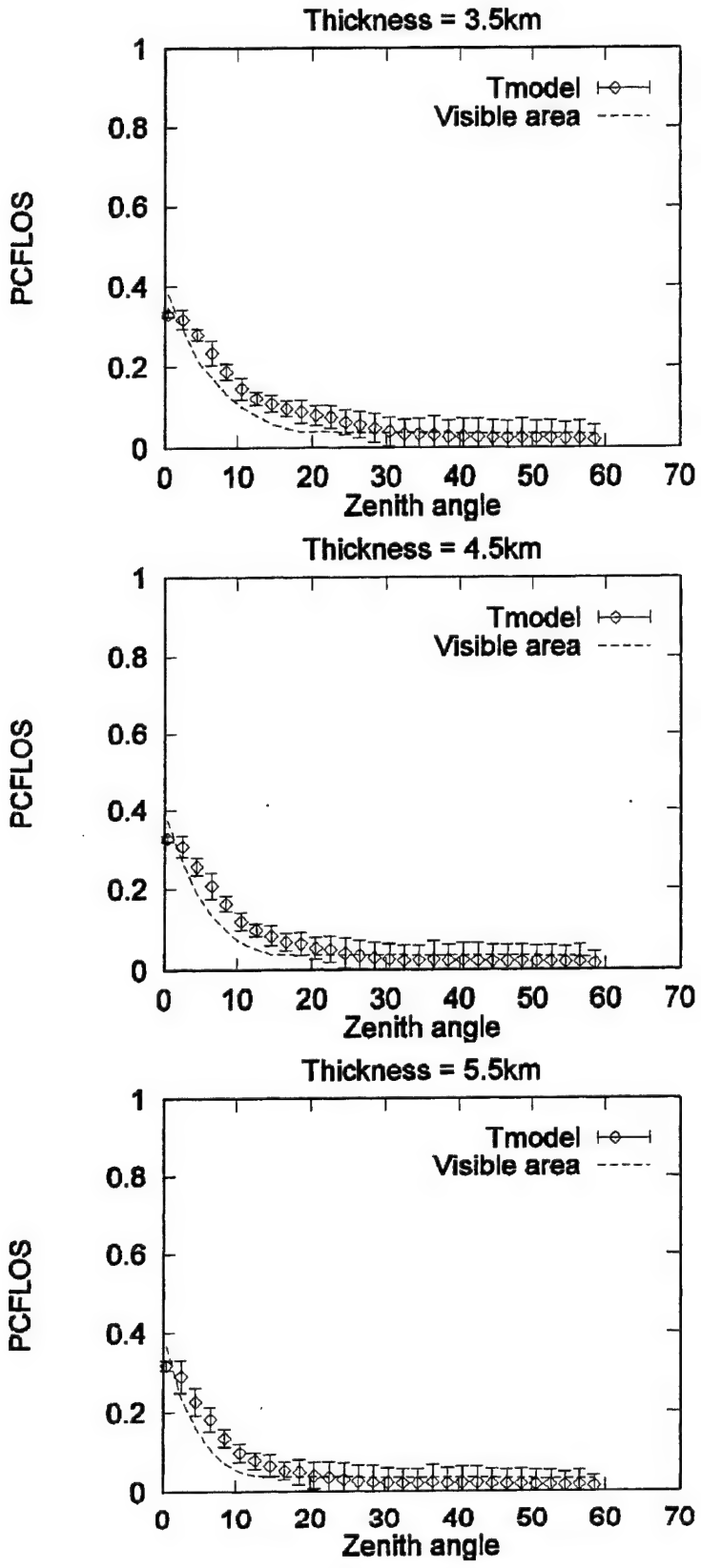

Figure 32. Visible Area Results for 60 Percent Coverage of Moderately Thick Clouds.

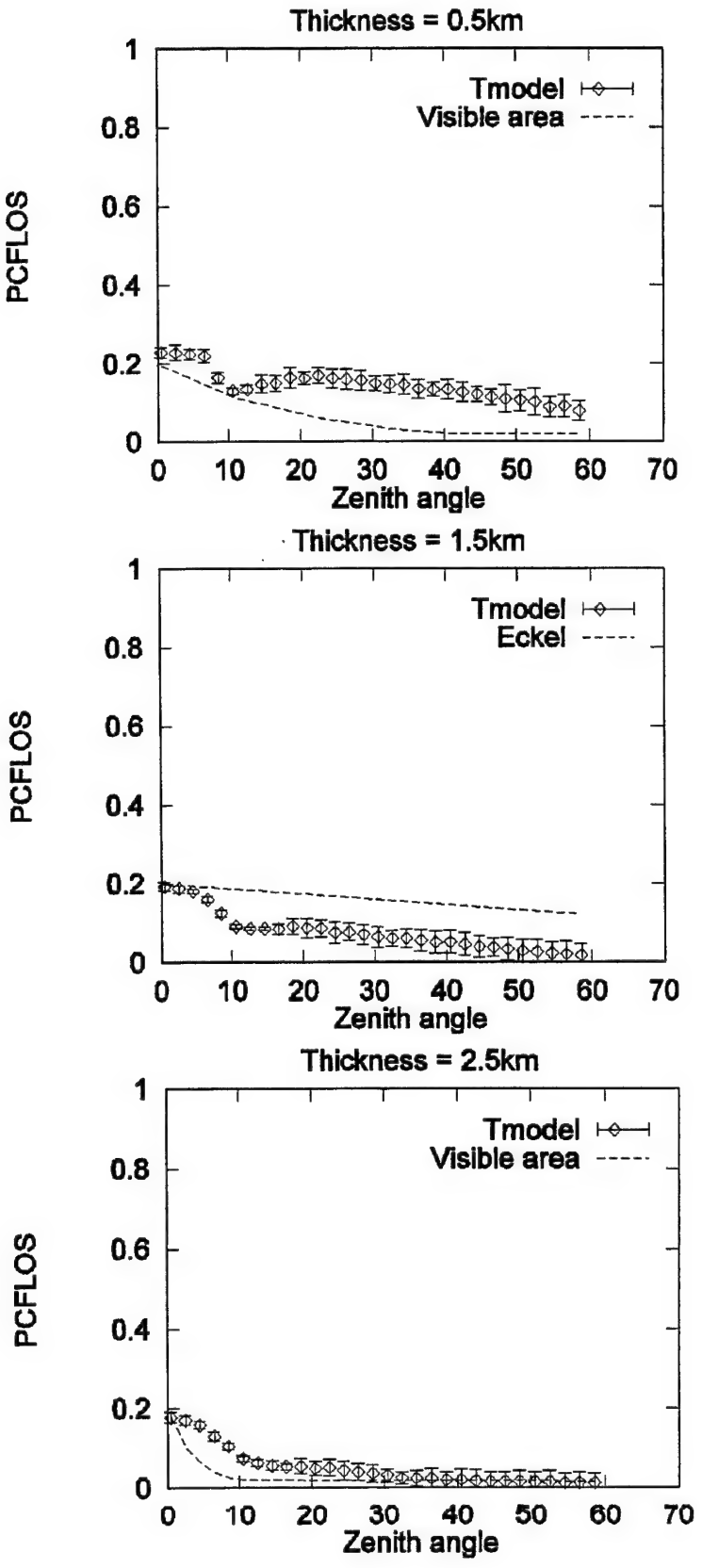

Figure 33. Visible Area Results for 80 Percent Coverage of Thin Clouds.

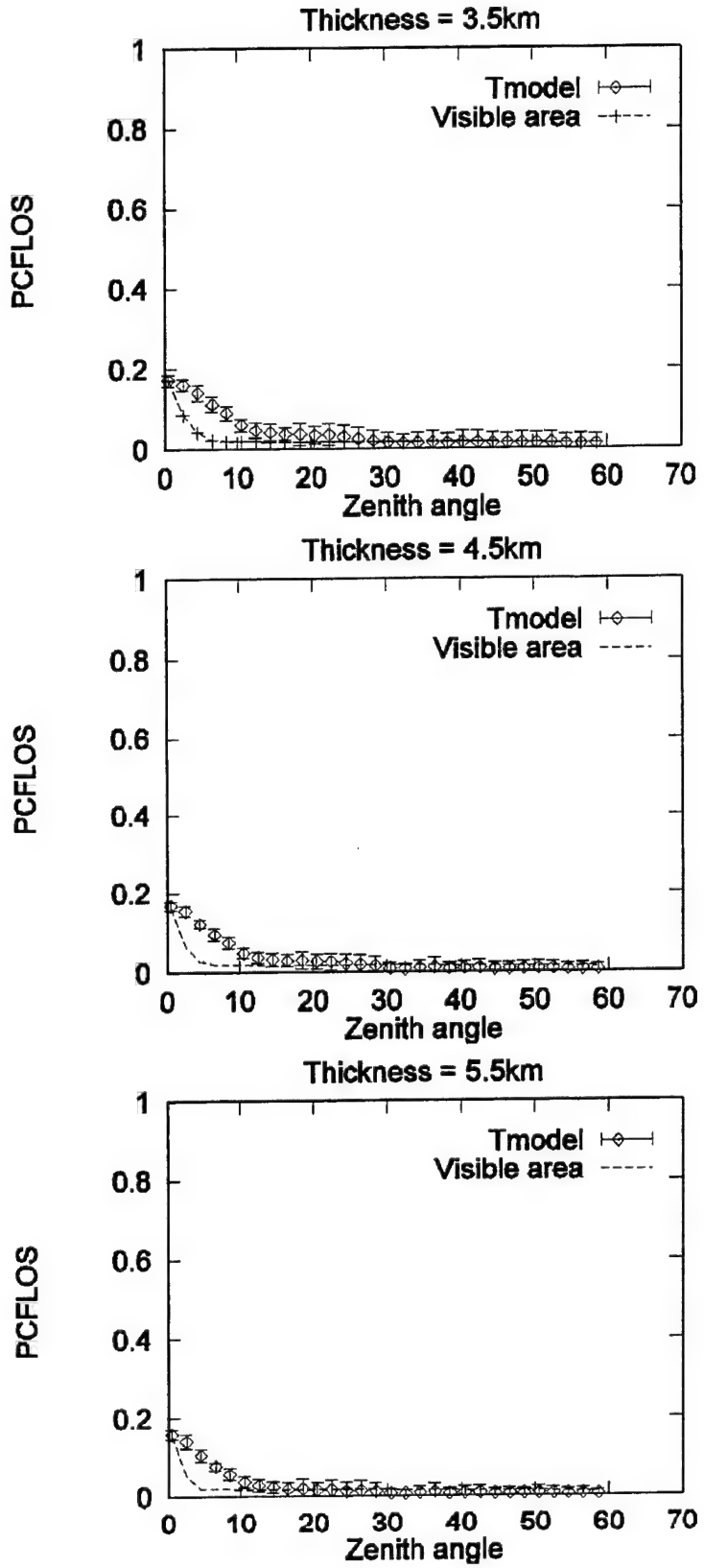

Figure 34. Visible Area Results for 80 Percent Coverage of Moderately Thick Clouds.

Results of the visible area model for cases that are not considered in the tuning process are shown in Figure 35. The PCFLOS values shown pertain to a cloud scene with 30 percent coverage and 3.0 km thickness and a range of zenith angles. Agreement is achieved between the visible area results and the hypercube results, also shown in the figure. This provides a measure of confidence in visible area results for arbitrary input values that are within the range of the tuning process.

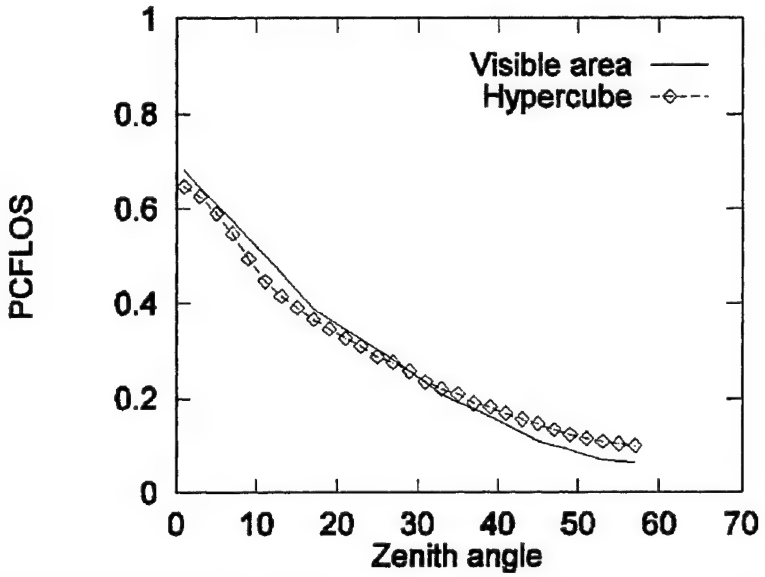

Figure 35. Visible Area Results for 30 Percent Coverage, 3.0 km Thickness With Hypercube Results.

4. ACTUAL PCFLOS MEASUREMENTS

Actual PCFLOS measurements are sought for comparison to model results. The only relevant data found that is extensive enough to be useful is that collected in [*Bertoni*, 1967]. An examination of this data shows that it would not be valuable to the present study. This is explained below, following a brief description of the data.

The Bertoni data is a collection of lines-of-sight (LOS) observations taken by flight crews. This data is referenced by other LOS studies and is discussed here for completeness. A total of 72,000 LOS observed at various elevations, angles, times of year, and locations (all within the northern hemisphere) were characterized as clear or not clear. The relative frequencies of clear LOS at different viewing angles are relevant to the present study. The angles at which observations were made are equivalent to zenith angles of 0°, 30°, 60°, and 90°. Observations were made both looking up and looking down.

The analysis of Bertoni's data led to some suspect results. For example, when the downward-looking observations for different locations and times of year were combined for altitudes between 20,000 and 40,000 ft, the frequencies of clear LOS were greater for a 60° zenith angle than for a 0° zenith angle. In addition, a subset of data pertaining to the San Francisco area indicated a higher probability of seeing blue sky directly above an observer at 30,000 ft than one at 40,000 ft. These results are contrary to the predictions of the detailed model, the proposed model, the Eckel model, and the expectations of the present authors.

The suspect results are unexplained; however, the subjectiveness of the observations and, in some cases, sample sizes, were contributing factors. The implication is that the data is unreliable in terms of relative frequencies of clear LOS at different viewing angles and altitudes. Therefore, the Bertoni data is not used to assess the models discussed in this study.

5. CONCLUSIONS

Two models are used to compute PCFLOS for a limited range of input values. One model performs detailed calculations based on physical and empirical considerations. This process is computationally expensive and therefore PCFLOS values are precomputed and stored in a hypercube, from which linearly interpolated values can be quickly obtained. Alternately, the visible area model proposed in this study can be applied to predict PCFLOS. This model is based on the geometry of LOS within a simplified, fictitious cloud scene. Tunable parameters required by the visible area model are evaluated for agreement with the detailed model and to reflect meteorological observations. The visible area model is computationally inexpensive but requires a set of detailed model results for tuning purposes. Both the visible area model and the hypercube approach to the detailed model are suitable for training and simulation purposes.

The detailed model is based on actual LOS through clouds generated with the Cloud Scene Simulation Model (CSSM) [*Cianciolo*, 1992; 1996] that generates realistic-looking clouds. A shortcoming of the detailed model results is that each PCFLOS value reflects a small number of specific cloud scenarios. Due to the wide variety of cloud arrangements that occur in nature and in the fictitious scenarios of the detailed model, it is difficult to identify or represent typical cases. Detailed model results would be improved if a greater number of cloud scenarios were incorporated and if cloud scenes were (subjectively) chosen to reflect a range of cloud features.

The visible area model uses several two-dimensional cloud scenes to represent each set of input values. A benefit of this approach is that the model outcome is not limited in the way that a single two-dimensional calculation would be, yet the model is only slightly more complicated than a single two-dimensional calculation. In other words, the averaging approach provides some measure of correction for the two-dimensional assumption. Averaging results of multiple calculations can be interpreted as combining results of several slices of a fictitious three-dimensional scenario.

The visible area model includes parameters that quantify cloud width. Due to the inherent difficulty in identifying typical widths, these parameters represent a range of widths and are subject

to tuning to meet specific requirements. In the present study tuning is done to produce agreement with the available detailed model results. A topic of interest for future work is determining the minimum detailed model results needed for tuning purposes. This could be compared to the number of detailed model runs required to populate a hypercube.

A comparison of detailed model results and Eckel model results indicate that Eckel model PCFLOS predictions are too large for moderately thick clouds. This suggests that the Eckel model does not capture the extent to which cloud thickness inhibits visibility.

6. RECOMMENDATIONS

The tools developed by this effort are appropriate for use in training simulations. The improvements to the detailed model discussed in Section 2.3 are significant but have not been subject to sufficient testing. Therefore, it is recommended that further testing of the improved version of the detailed model be carried out. The additional testing should include all of the cloud types that might be of interest and span an appropriate range of cloud thicknesses.

The visible area model may require retuning in consideration of the improved detailed model results that can now be generated. This should be done after (improved) detailed model results are available for a broader collection of clouds, including clouds at various altitudes and of various types. Note that the visible area model was developed for users who could not provide cloud type as input. Therefore, if multiple cloud types are available for tuning, then the detailed model results for different types must be combined to reflect typical PCFLOS values for a given altitude. Note, the visible area model could be modified to accept cloud type as input.

Both the visible area model and the detailed model have been used for spaces that can be described by a single set of input values. For example, the models do not capture the PCFLOS for a domain that is very different from its surroundings in terms of cloud coverage. This is particularly relevant to low look angles. Eckel handled this kind of environment by obtaining a PCFLOS value for each set of conditions and then combining the results. This method or one similar to it could be developed if the capability to model varying environments is needed. A numerical test of the outcome would be a comparison with detailed model results based on the appropriate combination of differing cloud tiles.

Experiments involving multiple cloud layers are recommended. A natural approach (and the one taken by Eckel) to multiple layers is to perform a PCFLOS calculation for each layer separately then use the product of the PCFLOS values to obtain PCFLOS for the multiple-layer scene. Such results should be compared to direct detailed model calculations for scenes with multiple layers.

Improvements in efficiency of detailed model runs would be worthwhile if a large number of runs is planned. For example, experiments with fewer missiles may show that the minimum number of missiles needed is less than 3000, the amount currently used. Prior to generating a new hypercube, some preliminary PCFLOS calculations can be done to determine efficient increments in

independent variables. In other words, how large can these increments be made without generating unacceptable levels of error due to linear interpolation from the hypercube?

The convenience and level of automation associated with the detailed model has evolved over the course of this study. A refinement that is planned for the next study is to have tmodel generate a warning when more tiles are required to prevent lines-of-sight to the missiles from going through the side of the cloud deck or missing the cloud deck completely.

REFERENCES

Bertoni, E. A., 1967, *Clear lines-of-sight from aircraft,* AFCRL-67-0435, Air Force Cambridge Research Laboratories, L. G. Hanscom Field, Bedford, MA, AD#657801.

Byers, H. R., 1944, *General Meteorology,* McGraw-Hill Book Co., Inc., New York.

Cianciolo, M. E., M. E. Raffensberger, E. 0. Schmidt, and J. R. Stearns, 1996, *Atmospheric scene simulation modeling and visualization*, PL-TR-96-2079, TASC, Reading, MA, ADA312179.

Cianciolo, M. E. and R. G. Rasmussen, 1992, *Cloud scene simulation modeling, the enhanced model,* PL-TR-92-2106, TASC, Reading, MA.

Eckel, A., 1999, *Modeling atmospheric effects on missile warning in the missile defense space tool,* Schriever AFB, CO.

Eckel, A. and J. Crane, 2000, $\mathbf{P_{CFLOS}}$ Project Status Report, Schriever AFB, CO.

WMO, 1969, *International Cloud Atlas 1969,* World Meteorological Organization, Geneva.

Kessler, E., 1986, *Thunderstorm Morphology and Dynamics,* University of Oklahoma Press.

Turkington, R. B., M. E. Cianciolo, and M. E. Raffensberger, 1998, *Atmospheric scene simulation modeling and visualization*, TR08607-1, TASC, Reading, MA.

APPENDIX. CALCULATION SUMMARY

This section summarizes the visibility calculation given in Section 3.3. Below are the input variables required for the visibility calculation:

θ	Zenith angle of interest $(0° \le \theta < 90°)$,
C	Fraction of cloud coverage,
B	Altitude of cloud base (km),
T	Thickness of cloud (km),
$\tilde{T}$	Thickness of cloud above altitude of interest (km).

Also, the following parameters are required:

n	number of cloud widths to consider,
L	length of the domain in km,
p_f	probability of a front.

Suggested values are n=4 and L=50. A simple choice for p_f is $1/(n+1)$. Other parameters have been assigned values in accordance with meteorological considerations. The calculation of visible area, v, is done by evaluating the functions listed below in the order of presentation.

Summary of Equations

Equation	Function	Variable	Parameters
(4)	b_l	(B)	β_l=4.0, B_l=2.0
(5)	b_h	(B)	β_h=4.0, B_h=6.0
(6)	t_g	(T)	τ=8.0, T_g=8.0
(7)	w^0	(b_l, b_h, t_g)	m^0, Δ_h^0, Δ_l^0, Δ_t^0
(8)	w^1	(b_l, b_h, t_g)	m^1, Δ_h^0, Δ_l^0, Δ_t^0
(9)	W_i, i=1, 2, …, n	(w^0, w^1)	n
(10)	θ_i^*, i=1, 2, …, n	$(C, \tilde{T}, W_i)$	n
(11)	vi, i=1, 2, …, n	$(C, \tilde{T}, W_i, \theta_i^*, \theta)$	n
(12)	W_{n+1}	(C)	L
(10)	θ_{n+1}^*	$(C, \tilde{T}, W_{n+1})$	
(11)	v_{n+1}	$(C, \tilde{T}, W_{n+1}, \theta_{n+1}^*, \theta)$	
(13)	v_f	(C, v_{n+1})	
(14)	PCFLOS	$(v_1, \ldots, v_n, v_f)$	p_f, n